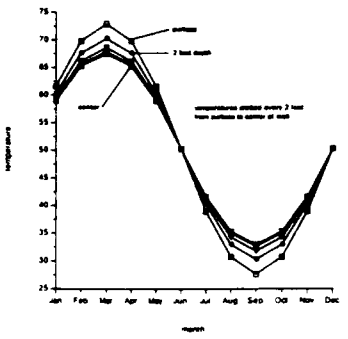

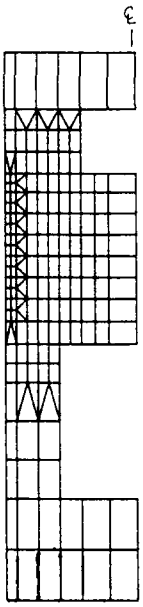

REPAIR, EVALUATION, MAINTENANCE, AND REHABILITATION RESEARCH PROGRAM

TECHNICAL REPORT REMR-CS-35

PREDICTING CONCRETE SERVICE LIFE IN CASES OF DETERIORATION DUE TO FREEZING AND THAWING

by

Larry M. Bryant, Paul F. Mlakar

JAYCOR
2734 Washington Street
Vicksburg, Mississippi 39180

March 1991
Final Report

Prepared for DEPARTMENT OF THE ARMY
US Army Corps of Engineers
Washington, DC 20314-1000

Under Contract No. DACW39-87-C-0059

Monitored by Structures Laboratory
US Army Engineer Waterways Experiment Station
3909 Halls Ferry Road, Vicksburg, Mississippi 39180-6199

The following two letters used as part of the number designating technical reports of research published under the Repair, Evaluation, Maintenance, and Rehabilitation (REMR) Research Program identify the problem area under which the report was prepared:

	Problem Area		Problem Area
CS	Concrete and Steel Structures	EM	Electrical and Mechanical
GT	Geotechnical	EI	Environmental Impacts
HY	Hydraulics	OM	Operations Management
CO	Coastal		

Destroy this report when no longer needed. Do not return it to the originator.

The findings in this report are not to be construed as an official Department of the Army position unless so designated by other other authorized documents.

The contents of this report are not to be used for advertising, publication, or promotional purposes. Citation of trade names does not constitute an official endorsement or approval of the use of such commercial products.

COVER PHOTOS:

TOP — Annual temperature cycles at various depths (above waterline).

BOTTOM — Finite-element thermal analysis model of middle wall.

REPORT DOCUMENTATION PAGE

Form Approved
OMB No. 0704-0188

1. AGENCY USE ONLY *(Leave blank)*	2. REPORT DATE	3. REPORT TYPE AND DATES COVERED
	March 1991	Final Report

4. TITLE AND SUBTITLE

Predicting Concrete Service Life in Cases of Deterioration Due to Freezing and Thawing

5. FUNDING NUMBERS

C DACW39-87-C-0059
WU 32412

6. AUTHOR(S)

Larry M. Bryant
Paul F. Mlakar

7. PERFORMING ORGANIZATION NAME(S) AND ADDRESS(ES)

JAYCOR
2734 Washington Street
Vicksburg, MS 39180

8. PERFORMING ORGANIZATION REPORT NUMBER

J650-89-002/1420

9. SPONSORING/MONITORING AGENCY NAME(S) AND ADDRESS(ES)

USAE Waterways Experiment Station
Structures Laboratory
3909 Halls Ferry Road
Vicksburg, MS 39180-6199

10. SPONSORING/MONITORING AGENCY REPORT NUMBER

Technical Report REMR-CS-35

11. SUPPLEMENTARY NOTES A report of the Concrete and Steel Structures problem area of the Repair, Evaluation, Maintenance, and Rehabilitation Research Program. Available from National Technical Information Service, 5285 Port Royal Road, Springfield, VA 22161.

12a. DISTRIBUTION/AVAILABILITY STATEMENT

Approved for public release; distribution unlimited

12b. DISTRIBUTION CODE

13. ABSTRACT *(Maximum 200 words)*

A probabilistic procedure was developed for prediction of service life of concrete structures subject to damage due to freezing and thawing and was applied to two typical Corps of Engineers' civil works structures. These hindcast applications demonstrate the procedure and provide results encouragingly comparable to observe deterioration. The sensitivity of the results to key material and environmental variables is discussed. Current testing procedures relevant to service life prediction are discussed along with recommendations for improvements in these areas.

14. SUBJECT TERMS

Concrete
Deterioration
Freezing and thawing
Reliability
Service life

15. NUMBER OF PAGES

79

16. PRICE CODE

17. SECURITY CLASSIFICATION OF REPORT	18. SECURITY CLASSIFICATION OF THIS PAGE	19. SECURITY CLASSIFICATION OF ABSTRACT	20. LIMITATION OF ABSTRACT
UNCLASSIFIED	UNCLASSIFIED	UNCLASSIFIED	

PREFACE

The work described in this report was authorized by Headquarters, US Army Corps of Engineers (HQUSACE), as part of the Concrete and Steel Problem Area of the Repair, Evaluation, Maintenance, and Rehabilitation (REMR) Research Program. The work was performed under Civil Works Research Work Unit No. 32412, "Predicting Concrete Service Life," for which Dr. Toy S. Poole, Concrete Technology Division (CTD), Structures Laboratory (SL), US Army Engineer Waterways Experiment Station (WES), was Principal Investigator. Dr. Tony C. Liu (CECW-EG) was the REMR Technical Monitor for this work.

Mr. Jesse A. Pfeiffer, Jr. (CERD-C) was the REMR Coordinator at the Directorate of Research and Development, HQUSACE; Mr. James E. Crews (CECW-OM) and Dr. Liu served as the REMR Overview Committee; Mr. William F. McCleese (CEWES-SC-A), WES, was the REMR Program Manager. Mr. James E. McDonald, CTD, SL, WES, was the Problem Area Leader.

The work was performed at JAYCOR, Structures Division, and this report was prepared by Dr. Larry M. Bryant, under the management of Mr. William J. Flathau. Technical guidance was provided by Dr. Paul F. Mlakar.

Dr. Poole, Cement and Pozzolan Group, Engineering Science Branch, was the Contracting Officer's Representative during the conduct and publication of the work and provided direct supervision. Technical support and review were provided at WES by Dr. C. Dean Norman, Ms. Sharon B. Garner, and Messrs. Michael I. Hammons and Anthony A. Bombich, CTD, SL. General supervision was provided by Mr. Kenneth L. Saucier, Chief, CTD, and Mr. Bryant Mather, Chief, SL.

Commander and Director of WES was COL Larry B. Fulton, EN. Technical Director was Dr. Robert W. Whalin.

CONTENTS

CONVERSION FACTORS, NON-SI TO SI (METRIC)
UNITS OF MEASUREMENT

Non-SI units of measurement can be converted to SI (metric) units as follows:

Multiply	By	To Obtain
inches	25.4	millimetres
feet	0.3048	metres
pounds (force)	4.448222	newtons
pounds (mass) per cubic foot	16.01846	kilograms per cubic metre
Btu	1.055	kilojoules
Fahrenheit degrees	5/9	Celsius degrees* or kelvins

* To obtain Celsius (C) temperature readings from Fahrenheit (F) readings, use the following formula: $C = (5/9)(F - 32)$. To obtain Kelvin readings, use $K = (5/9)(F - 32) + 273.15$.

PREDICTING CONCRETE SERVICE LIFE IN CASES OF DETERIORATION DUE TO FREEZING AND THAWING

PART I: INTRODUCTION

1. The Corps of Engineers (CE), in support of its navigation and flood control missions, must maintain the integrity of a large number of mass concrete structures. It often is necessary to evaluate the condition of the concrete in these structures to determine the magnitude and significance of specific problems, to assess the need for remedial action, or even to provide a basis for no action in conditions that might seem to indicate some action. A consistent and uniform procedure for predicting the service life of these concrete structures is necessary to properly allocate public funds for solution of identified problems. Such a procedure should reflect the current understanding of mechanisms which cause premature deterioration in concrete. It should incorporate available information concerning the concrete, environmental factors, and the current state of deterioration. In addition to incorporating what is known about these factors, the prediction of service life should reflect the uncertainties in knowledge of the foregoing factors.

2. A procedure for predicting the service life of concrete subject to damage by freezing and thawing which meets the above criteria has been developed and reported previously (Bryant and Mlakar 1988). This procedure addresses both the known and the uncertain qualities of the relevant material properties, environmental factors, and model of degradation due to freezing and thawing using a probabilistic method demonstrated in previous studies (Mlakar 1984) (Mlakar and Toussi September 1985, October 1985) (Bryant and Mlakar 1987). Two characteristics of this procedure which are natural requirements of such a method are: (1) the procedure rationally addresses the uncertainties inherent in the degradation of mass concrete due to freezing and thawing, and (2) the procedure is mathematically straightforward for implementation by CE offices.

3. Herein, this procedure is demonstrated by hindcast application to structural features at CE Civil Works structures. Three criteria were considered in reviewing potential candidates for application of the procedure. First, an appreciable degree of measurable damage due to freezing and thawing

of the feature was necessary to make a quantifiable comparison with the hindcast prediction. Next, the availability of data required for application of the procedure, e.g. temperature and concrete properties, was necessary for rational application. Finally, the selected candidate should be representative of typical CE projects. Six projects were initially considered as potential case study candidates - Dashields Locks and Dam, Emsworth Locks and Dam, Lower Monumental Lock Wall, Lockport Lock, and Locks 7 and 8 on the Monongahela. Two candidates which best met these criteria were selected as case studies for application of the procedure. These two candidates were the middle wall and land wall at Dashields Lock.

4. The procedure for predicting service life of mass concrete previously developed is reviewed in Part II of this report. The procedure is then applied to two case studies to demonstrate the procedure and determine the quantitative and qualitative results for real structures exhibiting damage due to freezing and thawing. In Part III, the procedure is applied to the vertical surface of the middle lock wall at Dashields Lock. Application of the procedure to the land wall at Dashields Lock is described in Part IV. The sensitivity of the probabilistic results to material and environmental factors is discussed in Part V. In Part VI, current and proposed testing requirements relevant to the prediction of concrete service life are discussed. Finally, our conclusions and recommendations related to this work are set forth in Part VII.

PART II: PROBABILISTIC PROCEDURE FOR PREDICTING SERVICE LIFE

Prediction Procedure

5. A probabilistic procedure for predicting service life of mass concrete subject to damage due to freezing and thawing was previously presented (Bryant and Mlakar 1988). The mechanism of freezing and thawing used in this procedure is based on the thesis that damage in a unit volume occurs when the temperature is below a critical value ($\theta < \theta_{cr}$) and the degree of saturation (amount of freezable water) exceeds a critical value ($S > S_{cr}$).[1] In a deterministic sense, this event is depicted in Figure 1, which indicates hypothetical time-histories of temperature and saturation in a unit volume of concrete. As seen in this figure, the temperature and degree of saturation vary in response to external environmental conditions as determined by the material properties. When either event occurs singly there is no damage but rather it is their simultaneous occurrence that causes damage. In this context, soundness of the concrete is considered a binary state process, i.e. either the unit volume is damaged or it is not.

6. The previous description of damage due to freezing and thawing is rational but deterministic. In fact, the temperature and degree of saturation in a structure vary randomly in time due to randomness of environmental conditions. As a consequence of the random nature of these conditions, the damage due to freezing and thawing and thus service life is also a random variable. In addition, the relevant material properties and critical values of temperature and saturation introduce additional uncertainty in the prediction of service life. Under these conditions, the hazard function or instantaneous rate of failure is:

$$h(t) = P\{\theta < \theta_{cr} \setminus S > S_{cr}\} \qquad (1)$$

that is, the joint probability of temperature less than critical and saturation greater than critical. Although the hazard function generally is a function of time, on the scale of damage due to freezing and thawing it is

---

[1] It should be noted that damage normally will occur only with non-air-entrained concrete.

reasonable to discuss annual failure rates, λ , which are unaffected by seasonal variations. For simplicity herein, we assume that the factors which determine criticality of temperature are independent of those defining the criticality of saturation such that:

$$\lambda = P(\theta < \theta_{cr}) \bullet P(S > S_{cr}) \tag{2}$$

7. The previous study demonstrated that the constant hazard function λ implies an exponential distribution of service life. Further, the expected service life is the reciprocal of the failure rate, i.e.:

$$T = 1/\lambda \tag{3}$$

It is obvious from Equations 2 and 3 above that an increase in the probability of temperature less than critical or saturation greater than critical increases the failure rate and inversely decreases the service life. The behavior implied by the above equations agrees with the observed deterioration history at typical CE concrete structures, i.e. some structures deteriorate rapidly and need early repair while others experience very slow deterioration. These extremes are indicated as λ_3 and λ_1 , respectively, in Figure 2. The primary interest of the Repair, Evaluation, Maintenance, and Rehabilitation Research Program is with intermediate cases with gradual but significant damage, such as that indicated by λ_2 in Figure 2.

8. In the discussion above, it is apparent that the probabilistic procedure includes four basic steps prior to determination of the required probabilities of temperature and saturation criticality for the unit volume. These steps are:

a. Determine critical temperature, θ_{cr} .

b. Determine critical degree of saturation, S_{cr} .

c. Determine distribution of temperature, θ .

d. Determine distribution of degree of saturation, S .

9. The critical temperature is a function of several factors which affect the freezability of water in the concrete. The impurities in the water reduce the freezing point below normal and, as any part of the water in

a pore begins to freeze, the remaining part has an even lower freezing point.* At this time these effects have not been quantified and, for the purposes of this study, a constant deterministic value of θ_{cr} will be assumed.

10. The critical degree of saturation is determined by a number of factors not known with certainty. Critical pore size, moisture migration due to freezing, and frost generated pressures are known to affect the critical degree of saturation. Currently, no widely accepted quantitative relationship between these variables is available. The previous study (Bryant and Mlakar 1988) suggested that a degree of saturation less than 91 percent is not critical, based on the 9 percent expansion of water when frozen.

11. Temperature in a unit volume can be estimated from the environmental conditions and thermal material properties. For some simpler cases, closed-form solutions of the deterministic heat transfer equations exist (Carslaw and Jaeger 1959). More generally, finite-element or finite-difference computer codes provide a solution (e.g. ADINA Engineering 1987). For the probabilistic analysis, we need to determine the distribution of temperature for the unit volume, as illustrated in Figure 3. In determination of this distribution, the uncertainty or randomness of the functionally independent variables in the deterministic analysis must be considered. In general, these random variables include environmental temperature θ_e , thermal conductivity k , specific heat c_p , and material density ρ .

12. Calculation of the degree of saturation experienced by a unit volume of concrete presents a more challenging problem, even in the deterministic sense. The previous study indicated that moisture migration in concrete is generally considered to include two mechanisms - seepage and capillary action.** Seepage through permeable materials is reasonably well understood and depends primarily on the coefficient of permeability of the material and the external heads of the fluid. On the other hand, capillary action is understood only conceptually, with little actual measurements or predictions

---

* Assuming the water is not a saturated solution before freezing begins - as it will be if nothing is dissolved in it but calcium hydroxide.

** In fact; for typical concrete having any value of water-cement ratio below 0.7, there will be no capillary continuity in concrete after 1 year; at lower valves continuity will be lost sooner, by 14 days for w/c = 0.5, hence moisture movement will be by surface diffusion in intact concrete.

available. For the purposes of these case studies, moisture migration, and thus degree of saturation, is computed only by considering the seepage mechanism. For the probabilistic analysis, we determine the distribution of degree of saturation for the unit volume, as illustrated in Figure 4. In determination of this distribution, the randomness of the functionally independent variables in the deterministic analysis, permeability and external head, are considered.

Environmental Data

13. The environmental data required for prediction of damage due to freezing and thawing by this procedure includes air temperatures, water temperatures, ground temperatures, and water levels. Each of these input random variables is described by a probability distribution function. The data for each variable was determined from an appropriate source for the case study site and represented by its statistical parameters.

14. For simplification of the input to the thermal analyses, the annual variations of air and water temperature were represented by a sinusoidal variation of temperature with an annual mean and amplitude. These variations are defined as:

$$\theta_a = A + B \sin(\omega t) + C \sin(\omega t) = A + D \sin(\omega t + \phi) \quad (4)$$

$$\theta_w = E + F \sin(\omega t) + G \sin(\omega t) = E + H \sin(\omega t + \phi) \quad (5)$$

where:

θ_a = Air temperature.

θ_w = Water temperature.

ω = Frequency = $2\rho/T$.

ϕ = Phase shift.

and A through H are constants determined by linear regression of a sinusoidal fit to the data, as described in Appendix A. An example of such data is in Table 1.

PART III: CASE STUDY OF MIDDLE WALL AT DASHIELDS LOCK

15. The first case study focused on the middle wall (between the two locks) at Dashields Lock on the Ohio River near Pittsburgh. The layout of Dashields Lock is shown in Figure 5, with a section through the middle wall shown in Figure 6. Key features of the middle wall include an access gallery in the top section and the filling and emptying gallery in the lower section. The wall is exposed to water in the lock chambers on both sides.

Temperature Criticality - Middle Wall

16. The air temperature data were obtained from Local Climatological Data provided by the National Oceanic and Atmospheric Administration (1986). For Dashields Lock, the air temperatures compiled for Pittsburgh, PA, were used due to its close proximity to the site. Average monthly air temperatures for Pittsburgh, shown in Figure 7, were the basis for the hindcast prediction.

17. Water temperature data at the site were obtained from the Ohio River Sanitary Commission. Water temperature data covering 4 years of daily measurement were downloaded from the STORET data base by US Army Engineer Waterways Experiment Station (WES) personnel. These data were synthesized into an annual temperature variation, shown in Figure 8, by averaging water temperatures of each calendar day over the 4 years.

18. Data were not available for annual variation of ground temperatures at the site. It was assumed that the ground temperature at the base of the lock could be reasonably represented as constant, and a value of 50° F was selected.

19. The temperature boundary conditions for thermal analysis of the middle wall are indicated in Figure 9. Above the mean waterline, the surface temperature was assumed to vary in sinusoidal fashion as shown in Figure 10. The temperature at the wall surface below the waterline was constrained to vary as shown in Figure 11. At the base of the structure, the ground temperature was assumed to remain constant at 50° F. The upper gallery was assumed open to the air and thus exposed to the air temperatures in Figure 10. The lower gallery, continuously filled with water, was therefore constrained to

water temperatures. The sinusoidal fits to the air and water temperatures according to Equations 4 and 5 produced the constants summarized in Table 1. The comparisons in Figures 10 and 11 confirm that this fit is a good representation of the actual data.

20. Calculation of temperatures for a unit volume of concrete was accomplished by using two analysis techniques, i.e., one-dimensional (1-D) and two-dimensional (2-D) models. The 1-D analysis uses an analytical solution of a slab with periodic temperature variation on each surface after Carslaw and Jaeger (1959) as indicated in Figure 12. For the periodic variation of external temperature θ_e, the attenuation of temperature with distance from the surface is predicted by the function $X(x)$ shown in the figure. As evident from this expression, temperature is a function of external temperature θ_e, distance from the surface x, and thermal diffusivity h^2. This attenuation of temperature with distance is indicated (for a unit θ_e) in Figure 13 for three typical values of thermal diffusivity.

21. Two 1-D thermal analyses of the wall were conducted for locations 2 ft above and below the waterline. The attenuation of temperature with depth, previously indicated in Figure 13, also indicates the sensitivity to thermal diffusivity. The annual temperature cycles above the waterline at depth intervals of 2 ft* are shown in Figure 14. This figure presents the same information as Figure 13 in a temporal format. An instructive look at calculation of the temperature distribution for a depth of 6 in. is presented in Appendix B. These sample calculations demonstrate the procedure for calculation of the deterministic temperatures and Taylor-series expansion for temperature distribution. A most important fact exposed by the calculation of the temperature distribution is the relative contribution of the various factors to the variance of temperature. The calculations indicate that, in this case, over 99 percent of the overall variance is due to the annual temperature amplitude, θ_a. This important factor was verified for all depths at the two locations above and below the waterline as shown in Appendix B. In all cases, the temperature amplitude accounted for over 97 percent of the overall variance. Thus, the uncertainties in other factors can be rationally ignored in

---

* A table of factors for converting non-SI units of measurement to SI (metric) units is presented on page 3.

further thermal analyses. This conclusion permits estimation of the overall temperature distribution with only a single deterministic analysis at the mean values, an extremely helpful factor in the 2-D analyses.

22. The 2-D finite-element model of the WES Concrete Technology Division (CTD) for the thermal analysis using the ABACUS program is illustrated in Figure 15. The symmetry of geometry and boundary conditions permitted analysis of only one-half of the wall, with a constraint of no heat flow across the plane of symmetry. The mesh is more highly discretized in the region of most interest and highest temperature variations, that is, along the wall surface near the waterline. A transient thermal analysis was conducted for a period of 3 years to obtain an annual cycle of temperatures at all nodal points in the wall. The 1-D analytical solution indicated that the effect of initial conditions would disappear after less than 1 year. Thus, the third year annual cycle was used to characterize the temperature distribution at any point in the wall.

23. At each location in both the 1-D and 2-D analyses, the mean and annual amplitude of temperature was obtained by fitting a sinusoidal curve to the computed annual temperature cycle. This curve fit was accomplished in the same manner as described in Appendix A for the environmental temperatures. An example of the curve fit is illustrated in Figure 16, which is shown for a typical node. The annual cycle of temperatures and the sinusoidal fit are shown to agree very well. A comparison of mean temperatures and annual amplitudes from the 1-D and 2-D analyses are compared in Figures 17 and 18 for the locations 2 ft above and below the waterline, respectively. As seen in these comparisons, the 1-D analyses predict reasonable values for both mean and amplitude, with the differences attributable to the actual 2-D nature of the problem. For example, above the waterline (Figure 17) the effect of the temperatures below the waterline is evidenced in the 2-D results but not in the 1-D results. The proximity of the warmer temperatures increases the mean temperature away from the air temperature boundary. The gallery reduces the annual temperature amplitude computed in the 2-D analysis. In effect, the gallery has the same effect as if the wall were actually less than 24 ft thick. Similar effects are seen in Figure 18 for the location below the waterline.

24. The annual probability of freezing at these two locations, according to the 1-D and 2-D analyses, is compared in Figure 19. Above the waterline, the probabilities range from about 20 percent at the surface to zero at 2.5 ft. Below the waterline, the temperatures never fall below 32° F. These comparisons instill confidence in the 2-D results and indicate that in some cases, 1-D analyses provide reasonable results.

25. The results of the 2-D thermal analysis are presented in detail for the area of the wall indicated in Figure 20. The computed mean temperature levels are contoured in Figure 21. As expected, the mean temperatures near the surface reflect the mean air and water temperatures and transition between these extremes. The annual amplitudes of temperature are depicted for this area in Figure 22. Near the surface, the amplitudes are near those of the air and water temperatures, which are almost the same. In addition to the expected reduction of amplitude with distance from the surface, the effect of the upper and lower galleries is evident in this plot. As the surfaces of the gallery walls are exposed to the same temperature variations as the outer surfaces, the temperature amplitudes near these surfaces tend to have higher values. Probability of freezing in this area of the wall is illustrated in Figure 23. As should be expected, the probability of freezing is zero below the waterline and for some interior portions above the waterline. The probability of freezing above the waterline is primarily driven by the reduction of temperature amplitude with increasing depth.

Saturation Criticality - Middle Wall

26. As noted in Part II, determination of degree of saturation in concrete is a complex problem considered to embody two methods of moisture migration - seepage flow and capillary action. Although there have been attempts in the past to estimate height of capillary rise in various soils, these estimates are extremely approximate and do not extend to other materials such as concrete. For the purposes of these case studies, moisture migration was considered to occur by seepage alone. Further, although 2-D finite-element and finite-difference solutions for seepage exist, a simpler solution to this essentially steady-state problem was applied. This approach, depicted in Figure 24, reflects a steady-state location of the phreatic surface in a

surface in a concrete wall for a given set of boundary conditions (external head). Essentially, in this case, the phreatic surface is along a straight line between the water levels on each side of the wall. Attendant to this assumption is the recognition that the material is fully saturated along and below the phreatic surface and unsaturated above it. The seepage model gives no information on the expected variation of degree of saturation above the phreatic surface. Thus, the location of 91 percent saturation cannot be determined from the seepage model. Therefore, for these case studies, the degree of saturation is considered critical below the phreatic surface and not critical above.

27. The water levels in a lock were characterized by a mixed distribution shown in Figure 25. This distribution is based on normal distributions with means at high and low pool elevations of 690 and 684 ft, respectively, with a standard deviation about each mean of 6 in. The combined distribution assumes equal probability of high or low pool and is adjusted to maintain a maximum probability of unity. As the water levels on each side of the wall have the same distribution, the location of the phreatic surface, and thus the location of critical saturation, has the same distribution as the water level. Attendant to this observation, the probability of critical saturation is as shown in Figure 26. This plot reflects the cumulative distribution function (CDF) of Figure 25. It should be noted from the CDF that the probability of critical saturation is a constant 50 percent from about elevation 685 to 689 ft.

Material Service Life - Middle Wall

28. As a preliminary step in calculation of the service life, the annual hazard function is computed as described by Equation 2. This hazard function is depicted for the central section of the middle wall in Figure 27. As defined by Equation 2, this figure is the product of Figures 23 and 26. As should be expected, the highest probability of damage (the hazard function) is near the wall surface just above the waterline. This is the area of higher probabilities of critical saturation and critical temperatures. Naturally, the area below the waterline and near the interior of the wall has essentially no chance of damage since the temperatures have little chance of being below

critical in these areas. As seen in Figure 26, the probability of saturation is nil more than 2 ft above the mean high pool, thus the hazard function is likewise nil in this area.

29. The material service life for degradation due to freezing and thawing is estimated for the middle wall according to Equation 3. This function, the inverse of the hazard function, is plotted in Figure 28. As seen in this plot, the service life is predicted to be only 15 years at a depth of 9 in. At 2 ft, the service life is predicted to be about 40 years, with a service life of about 100 years at 3 ft.

30. This service life prediction (hindcast, actually) is encouragingly similar to the observed deterioration on the middle wall at this site. Measurements of damage due to freezing and thawing in the middle wall made by the WES (1986) in 1980 indicated depths of deterioration of 0 to 2 ft. Given the fact that the lock was constructed in 1927-1929, the measurements of damage after 50 years are very close to those hindcast by this procedure, although damage rates on this structure were affected by at least two additional factors. One, some repair work (shotcrete overlays) would tend to reduce rate of damage. Two, abrasion by barges would tend to enhance the rate of damage.

PART IV: CASE STUDY OF LAND WALL AT DASHIELDS LOCK

31. The second case study was the land wall at Dashields, previously shown in Figure 5. A section through the land wall, shown in Figure 29, serves to indicate the similarities and differences of the land wall and the middle wall. The wall is of similar construction with a maximum thickness of 24 ft and having similar upper and lower galleries. The wall is not symmetric, stepping down to a minimum thickness of 12 ft in the upper section. The other primary difference between the two walls lies in the boundary conditions. Obviously, the river side of the land wall is exposed to similar temperature and moisture conditions as the middle wall. The land side of the wall, being in full contact with the ground, is exposed to different temperature and moisture conditions.

Temperature Criticality - Land Wall

32. The temperature boundary conditions for thermal analysis of the land wall are indicated in Figure 30. Along the river side of the wall and the upper and lower surfaces, the temperature boundary conditions shown are the same as for the middle wall. Temperatures in the upper and lower galleries were likewise constrained to the ambient air and water temperatures, as in the analysis of the middle wall. The temperatures along the land side of the wall obviously must vary between the annual air temperature cycle at the surface and the constant ground temperature at the base. In order to estimate this variation, a 1-D analysis of the ground as a semi-infinite medium exposed to cyclic temperature variation at the surface was performed as described by Carslaw and Jaeger (1959). This 1-D analysis produced the results shown in Figure 31. These results indicate that the cyclic temperature effect has an effect only for about the top 5 ft of the ground. Below this depth, the nature of the cyclic air temperature has essentially no effect. For comparative purposes, the results are compared with those for a typical concrete.

33. In the finite-element thermal analysis by the CTD, a portion of the soil was modeled in an attempt to better define the appropriate thermal conditions along the land face of the wall. The finite-element model, shown in Figure 32, included a representation of the soil out to a distance of

30 ft from the wall at the ground surface (18 ft at the base). As seen in Figure 32, an adiabatic boundary (no heat flow) was specified vertically to an elevation of 680 ft with constant ground temperatures (50° F) specified for the remainder of the depth Ambient air temperatures were specified along the ground surface. This soil portion of the model was felt to better represent actual temperature gradients along the land face of the wall. The results near the river face of the wall, where temperature and saturation criticality were most important, are not likely to be much affected by this boundary condition.

34. The thermal analysis was conducted by the WES CTD using the ABACUS computer code for the land wall given the above boundary conditions. In this case, the entire model was analyzed, since there was no symmetry as in the middle wall. As for the analysis of the middle wall, a transient analysis for 3 years was conducted, and the nodal temperature results of the third year were used to characterize the sinusoidal distribution of internal temperatures. This analysis produced the contours of mean temperature, shown in Figure 33, and the annual variation of temperature, shown in Figure 34, for the central portion of the lock wall. As was seen in the middle wall, the mean temperatures and annual amplitudes track the ambient conditions near each surface and transition rather smoothly in this section. The probability of temperature being critical, for simplicity of agreement taken to be below 32° F, varies from zero to about 0.18 in this region, and is plotted in Figure 35. The probability of freezing exists only above the waterline, and generally decreases with distance from a surface exposed to the air.

Saturation Criticality - Land Wall

35. The saturation model for the land wall is quite similar to that for the middle wall, recognizing the difference in water levels on both sides of the lock wall. As for the middle wall, the water levels in the lock were characterized by the mixed distribution shown in Figure 25. The actual distribution of water table elevation on the land side of this wall is not known. However, piezometer data was available for three locations along the land wall for a period of about 4 years. This transient data for the piezometer near the middle of the lock is plotted in Figure 36 for this period.

For the purposes of the case study, it was reasonable to assume that the land side water table fluctuated much more slowly than the lock pool elevation and that it could be reasonably represented by an average water table elevation, also indicated as about 690 ft in Figure 36. As the phreatic surface was assumed to lie along a line between the water levels on each side of the wall (as for the middle wall), the resulting distribution of this surface, and thus the probability of critical saturation, is as depicted in Figure 37. Essentially, the distribution at the river side of the wall (shown in Figure 25) is mapped through the depth of the wall, decreasing to the point distribution at the land face of the wall. Thus, the distribution at any distance from the surface is identical, but acts over a smaller range of elevation. The probability of critical saturation was computed at every point in the wall corresponding to the nodal points in the thermal analysis, and this probability is plotted in Figure 38. This contour plot reflects the mapping of the pool elevation distribution at the river side to the constant, mean water table elevation at the land side.

Material Service Life - Land Wall

36. The annual hazard function, as defined by Equation 2, is depicted for the central section of the land wall in Figure 39. Once again, the highest probability of damage is near the wall surface just above the water-line. This is the area of higher probabilities of critical saturation and critical temperatures. The area below the waterline and near the interior of the wall has essentially no chance of damage since the temperatures have little chance of being below critical in these areas. As was seen in Figure 38, the zero probability of saturation more than 2 ft above the mean high pool produces a zero probability of damage in this area.

37. The material service life for degradation due to freezing and thawing for the land wall is estimated according to Equation 3, and is plotted in Figure 40. As seen in this plot, the service life is predicted to be only 15 years at a depth of about 6 in., with service life about 75 years at 2 ft.

38. This service life prediction is generally similar to the observed deterioration on the land wall at this site. Specifically, measurements of damage due to freezing and thawing in the land wall (WES 1986) in 1980

indicated depths of deterioration generally somewhat less than along the middle wall. The constraining effect of the relatively constant ground temperatures and the thinner upper section of the wall reduced the area subject to critical temperatures in the land wall. As a result, the probability of damage is reduced, and the expected service life increased in the land wall.

PART V: SENSITIVITY TO KEY MATERIAL AND ENVIRONMENTAL VARIABLES

Temperature Distribution

39. The calculations presented in Appendix B provided an instructive look at calculation of the Taylor-series expansion for temperature distribution. An important fact revealed by this calculation of the temperature distribution was the relative contribution of the various factors to the variance of temperature. The calculations indicated that, for a depth of 6 in., over 99 percent of the overall variance is due to the annual temperature amplitude. In fact, the temperature amplitude accounted for over 97 percent of the overall variance for all cases evaluated in the 1-D analyses. This fact indicated that the uncertainties in other factors could be rationally ignored in the thermal analyses. This conclusion permitted estimation of the overall temperature distribution with a single deterministic analysis at the mean values. In terms of sensitivity, the temperature distribution is sensitive only to the annual amplitude of temperature. Uncertainty in other factors did not significantly contribute to uncertainty of internal concrete temperatures.

Saturation Distribution

40. The estimation of the degree of saturation in the concrete was based on three general assumptions. First, the water level in the lock was assumed to follow the distribution previously indicated in Figure 25. This mixed distribution assumes two normal distributions centered about the nominal high and low pool elevations, which are the nominal high and low water elevations in the lock. A reasonable standard deviation about these two means was assumed to represent fluctuations in the two pool elevations. This distribution reflects the assumption that the water in the lock is left at whatever level exists when the exit gate is closed until the next lockage occurs. Since there was no evidence to the contrary, it was assumed that there was an equal probability of downstream or upstream traffic, and thus the two normal distributions are weighted equally.

41. The second general assumption in development of the degree of saturation involved the method of moisture migration and the procedure used to

determine the degree of saturation. Moisture migration was assumed to occur primarily by seepage. For the problem at hand with small differences in external heads, the phreatic surface lies essentially on a straight line between the external water levels, and the straight line surface was utilized in the analysis.

42. The third assumption in determination of saturation criticality was that the phreatic surface (100 percent saturation) defined the boundary of critical saturation. The seepage analysis for unconfined flow provides only this surface and does not predict where a lesser degree of saturation, such as 91 percent, exists. For the purposes of this study, this effect was felt to be small.

43. For the assumptions of this study, the primary uncertainty in degree of saturation and probability of critical saturation resides totally in the assumed distributions of external head. Other uncertainties not considered in this study might be as important as external head and are worthy of additional study.

PART VI: TESTING FOR SERVICE LIFE

44. The procedure presented herein for prediction of concrete service life presumes the availability of information regarding environmental conditions, thermal and permeability properties of concrete, and methods to compute the response of the structure for these conditions. In addition to knowing expected or mean values of the input variables, the uncertainty associated with each is also needed. The current availability of this information indicates that physical testing is warranted to improve the knowledge in some areas.

45. Experimental work supporting prediction of concrete service life obviously includes measurement of temperature and moisture content of concrete by both laboratory and in-situ testing. Experimental work in these areas can provide valuable information in two different, but related forms. First, physical tests can provide first-hand information and data regarding the actual conditions at a site for evaluation of the condition of the concrete. Second, and important for the long-term improvement of service life prediction, these measurements can provide validation for analytical methods of temperature and moisture prediction.

Temperature

46. Measurements of temperature for prediction of concrete service life would be most appropriately obtained by in-situ testing. Temperature measurements are required both for the external conditions, such as air, water, and ground temperatures, and internal to the structure itself. These measurements should be made on a long-term basis, i.e. over a period of years, to evaluate the external temperatures and the thermal response of the structure. Current procedures and measurement devices are certainly adequate to provide this information. The major difficulty in thermal measurement lies in the difficulty in delivery or placement of these devices internal to existing structures. Methods to place thermocouples in a structure with minimal cost and minimal disturbance of the structure and its function should be the primary concern at this time. The measurement and recording devices should also provide sufficient reliability to provide accurate measurements over the

period of years required to accumulate the necessary data. Analytical studies of the thermal response of the structure should be an integral part of the test planning to insure appropriate, strategic placement of gages.

Saturation

47. Evaluation of degree of saturation in concrete should be considered in both in-situ and laboratory tests. Core samples removed from a subject structure can be sealed to minimize moisture migration and tested in a laboratory. A current American Society for Testing and Materials (ASTM) procedure, ASTM C 642-82 (ASTM 1989) could provide a basis for laboratory determination of degree of saturation in concrete. This procedure currently addresses measurements for specific gravity, absorption, and voids in hardened concrete. Two slight modifications of the procedure would allow estimation of in-situ degree of saturation. First, the specimen should be sealed with a relatively impermeable coating immediately after removal from the structure to prevent drying or wetting of the concrete. After this coating is removed in the lab, the mass of the specimen should be recorded. The remainder of the procedure, including complete drying and saturation of the specimen, would remain as specified in the standard. The in-situ degree of saturation could then be computed from the original mass, dry mass, and fully saturated mass as:

$$S = (W_0 - W_d)/(W_s - W_d) \quad (6)$$

where:

S = Degree of saturation, percent.

W_0 = Original specimen mass.

W_d = Dry specimen mass.

W_s = Saturated specimen mass.

This modified procedure should provide a reasonable estimation of the actual degree of saturation in the structure at the location of the specimen.

48. In-situ measurements for degree of saturation are expected to provide considerably more challenges than those for temperature. Measurements of external factors, such as water levels and rainfall amounts, should be

attainable using currently available technology. The major consideration in these measurements would be the long-term reliability of the measuring and recording devices. A first cut at measurement of saturation in a concrete structure would probably reflect the current technology in measurement of moisture in other media such as soil. That is, an arrangement of piezometric devices might be able to provide an estimate of the location of the phreatic surface over a period of time. In the long run, nonintrusive measurement procedures that can detect moisture migration would be highly desirable.

49. An initial goal of physical testing for degree of saturation should be the validation of current theories and models for moisture migration. This goal can probably be approached through small-scale or laboratory simulations that consider both seepage and capillary action.* Validation of an existing or new model for moisture migration would be an important step in improvement of service life in concrete.

---

* or diffusion; see e.g. Bremer, H. W. 1965. "Moisture Migration - Concrete Slab-on-Ground Construction," Journal of the PCA Research and Development Laboratories, May, pp 2-17, also PCA Development Dept. Bulletin D 89 and references given therein; also Powers, T. C.; L. E. Copeland, and H. M. Mann. 1959. "Capillary Continuity or Discontinuity in Cement Pastes," ibid May pp 38-48, also PCA Research Laboratory Bulletin 110 and references given therein.

PART VII: SUMMARY, CONCLUSIONS, AND RECOMMENDATIONS

Summary

50. A procedure for predicting the service life of nonair-entrained concrete subject to damage due to freezing and thawing has been developed which addresses both the known and uncertain qualities of the relevant material properties, environmental factors, and model of degradation due to freezing and thawing using a probabilistic method. Two important characteristics of this procedure are: (1) it rationally addresses the uncertainties inherent in degradation of mass concrete due to freezing and thawing, and (2) the procedure is mathematically straightforward for implementation by CE offices.

51. This procedure was demonstrated by hindcast application to two structural features at CE Civil Works structures which exhibited an appreciable degree of measurable damage due to freezing and thawing. Required data for application of the procedure, e.g. temperature and concrete properties, were available for these features, which were representative of typical CE projects. From six candidate structures, two features were selected as case studies for application of the procedure. These two features were the middle wall and land wall at Dashields Lock.

52. The procedure was applied using the available data for each case study. One- and two-dimensional thermal analyses were used to determine the thermal response of each wall and the resulting probabilities of critical temperature. Simplified seepage analyses provided the probabilities of critical saturation. The annual probability of damage and the predicted service life were determined from the joint probabilities of critical temperature and critical saturation throughout the structure.

53. Sensitivity of concrete service life prediction to the uncertainties of input factors was discussed. Implications of physical test procedures, and discussion of future needs for concrete service life prediction were examined.

Conclusions

54. Several important conclusions can be reached from this study. Current procedures for thermal modeling and analysis appear quite adequate for predicting temperatures in a concrete structure. Although 2-D analyses are better for determining complex thermal response, in many cases a series of much simpler 1-D analyses provide a very good estimation of temperatures. The external temperature inputs to a thermal analysis, i.e. water and air temperatures, were shown to be well represented by sinusoidal curves. In this respect, the internal thermal response of a unit volume of concrete likewise follows a sinusoidal variation. This observation permits a simplified representation of the inputs and results of the thermal response, and also simplifies application of 1-D analyses. An examination of the temperature distribution for any point in the structure indicated that the primary contributor to uncertainty of response was the annual variation of temperature. This important observation permits the probabilistic analysis to use the results of only a single thermal analysis at the mean values of the input factors.

55. The general understanding and analytical models for predicting moisture migration and degree of saturation are not as well developed as for the thermal problem. A seepage model for predicting the degree of saturation appears to provide adequate answers for the prediction of service life; however, further study is appropriate to substantiate this indication.

56. The procedure developed and presented herein provides excellent agreement with observed damage due to freezing and thawing at the two sites studied. The general trends of location and spatial variation of damage are very similar to observations and measurements at the two sites. More encouragingly, the actual magnitudes of damage predicted by the procedure compare favorably with the previous measurements. This result provides the strongest indication that the procedure is rational and would enhance the ability of the CE to predict service life at its many other concrete structures.

Recommendations

57. This study provides a strong basis for prediction of concrete

service life at typical CE structures, but would be strengthened considerably by investigating several areas exposed by the study. Based on the extremely favorable results of the two case studies of this study, the procedure should be applied to several other structural features typical to CE structures for which actual damage is reasonably well known. These additional applications of the procedure would likely increase the confidence in the procedure and indicate any areas that require refinement before broad application to structures without damage measurements. As a precursor to these additional applications, a small survey of structural features and extent of damage due to freezing and thawing would indicate the most appropriate structures to consider.

58. The current understanding (or lack of understanding) of moisture migration in concrete structures indicates some further development of models for moisture migration is warranted. This development would include more extensive review and examination of the current theories and their applicability to the problem at hand.

59. As a natural adjunct to the further refinement of the procedure, the procedures for physical measurements of temperature and moisture should be extended to provide direct information regarding structure state and validation for the analytical models. This extension is relatively straightforward for thermal measurements but will likely require some innovative improvements for measurement of moisture.

REFERENCES

ADINA Engineering. 1987. "Automatic Dynamic Incremental Nonlinear Analysis - T," Users Manual, Report ARD 87-2, Watertown, MA.

American Society for Testing and Materials. 1989. Annual Book of ASTM Standards, Section 4, Vol 4.02, Philadelphia, PA.

Bryant, L. M. and Mlakar, P. F. 1987. "Evaluation of Civil Works Steel Structures," Report No. J650-87-003, prepared by JAYCOR, Vicksburg, MS, under Contract No. DACW88-86-R-0007 for the US Army Construction Engineering Research Laboratory, Champaign, IL.

Bryant, L. M. and Mlakar, P. F. 1988. "Concrete Service Life," Report No. J650-88-003, prepared by JAYCOR, Vicksburg, MS, under Contract No. DACW39-87-C-0059 for the US Army Engineer Waterways Experiment Station, CE, Vicksburg, MS.

Carslaw, H. S. and Jaeger, J. C. 1959. 2nd ed., Conduction of Heat in Solids, Clarendon Press, Oxford.

National Oceanic and Atmospheric Administration. 1986. "Local Climatological Data, Annual Summary with Comparative Data," National Climatic Data Center, Asheville, NC.

Mlakar, P. F. 1984. "A Statistical Study of the Condition of Civil Works Steel Structures," Report No. J650-84-001, prepared by JAYCOR, Vicksburg, MS, under Contract No. DACW88-84-M-1221 for the US Army Construction Engineering Research Laboratory, Champaign, IL.

Mlakar, P. F. and Toussi, S. September 1985. "Reliability of Civil Works Structures: General Methodology and Application to Sheet Piles," Report No. J650-85-003, prepared by JAYCOR, Vicksburg, MS, under Contract No. DACW88-85-C-0010 for the US Army Construction Engineering Laboratory, Champaign, IL.

_____. October 1985. "Hazard Function for Miter Gates," Report No. J650-85-005, prepared by JAYCOR, Vicksburg, MS, under Contract No. DACW88-85-C-0011 for the US Army Construction Engineering Research Laboratory, Champaign, IL.

US Army Engineer Waterways Experiment Station. 1986. "Condition Survey, Lower Monongahela and Upper Ohio, Dashields Locks and Dam, Ohio River," Structures Laboratory, Vicksburg, MS.

Table 1

Constants From Sinusoidal Fit of Temperature Data

Linear Regression of Air Temperature Data (Equation 4):

Air temperature, $\theta a = A + B \sin(\omega t) + C \cos(\omega t)$

$= A + D \sin(\omega t + \phi)$

$A = 50.275°$ F

$B = -7.972°$ F

$C = -21.187°$ F

$D = 22.637°$ F

Linear Regression of Water Temperature Data (Equation 5):

Water temperature, $\theta w = E + F \sin(\omega t) + G \cos(\omega t)$

$= E + H \sin(\omega t) + \phi)$

$E = 56.538°$ F

$F = -9.387°$ F

$G = -20.018°$ F

$H = 22.110°$ F

Table 2

Horizontal Depth of Freeze-Thaw Damage in Dashields Lock Walls

		Typical Lock Wall		Lower Gate Recess	
Wall	Side of Wall	Monolith No.	Depth of Damage ft	Monolith No.	Depth of Damage ft
River	Land	L-18	0.0	L-33	1.5
		L-19	0.2	L-34	1.2
		L-24	0.0	L-35	1.3
		L-28	0.0		
		L-30	???		
Middle	River	M-11	0.0	M-22	0.6
		M-12	0.1	M-23	2.8
		M-16	0.1	M-24	2.9
		M-19	0.8		
	Land	M-12	???	M-20	0.3
		M-16	???	M-21	0.1
Land	River	R-13	1.2	R-24	0.4
		R-20	0.6	R-24	1.0

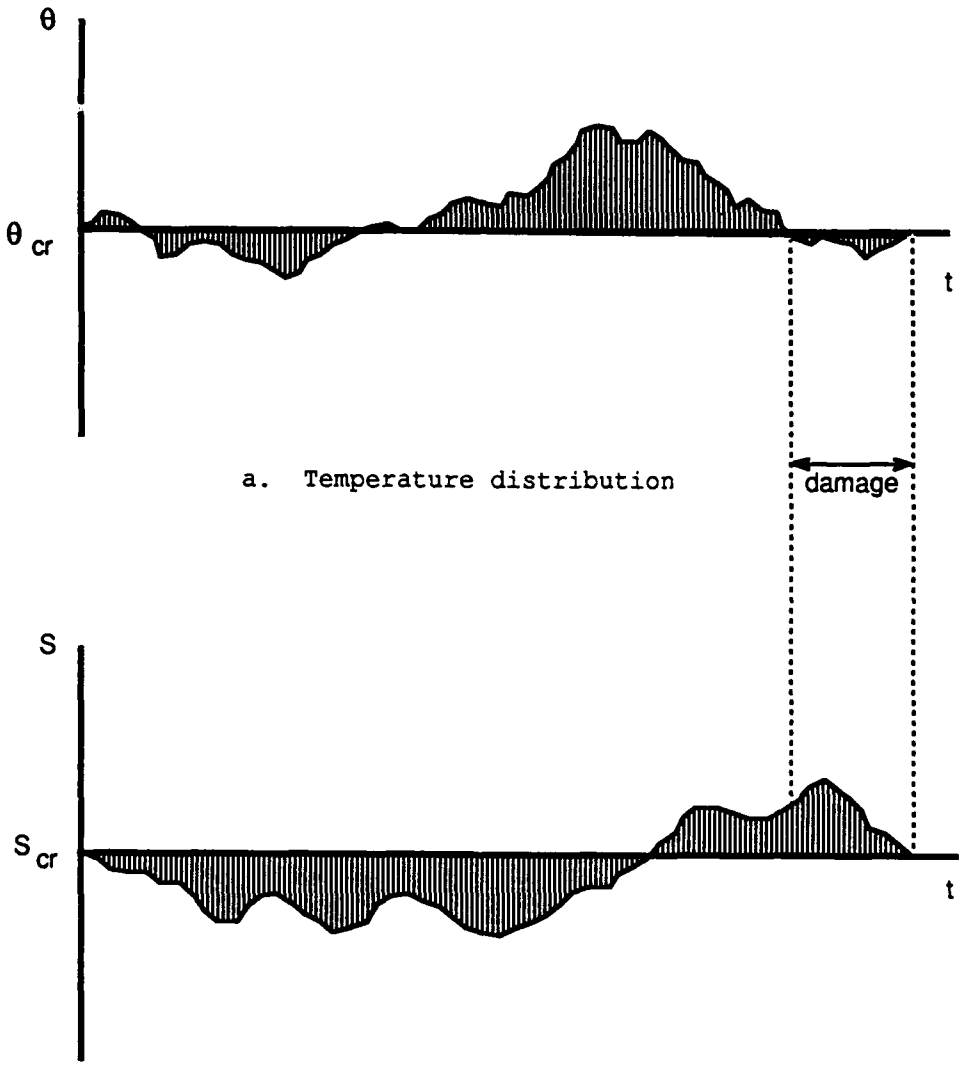

a. Temperature distribution

b. Saturation distribution

Figure 1. Determine mechanism of damage by freezing and thawing

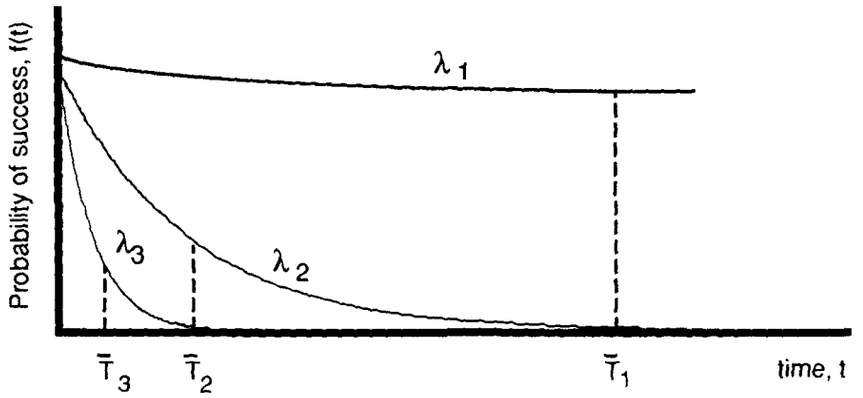

a. Probability density function.

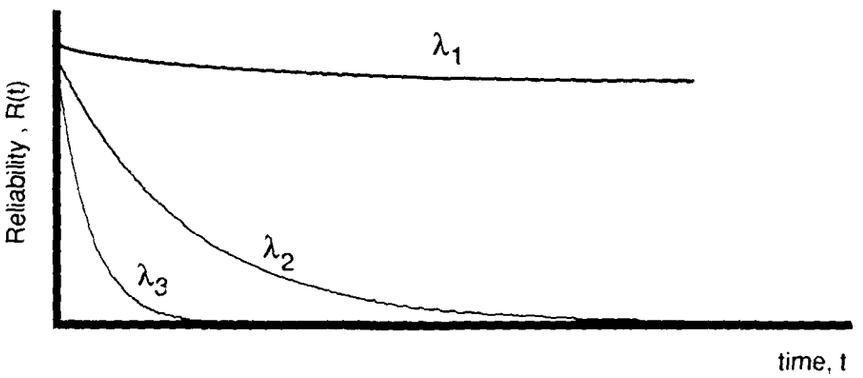

b. Reliability function.

Figure 2. Distribution of material service life

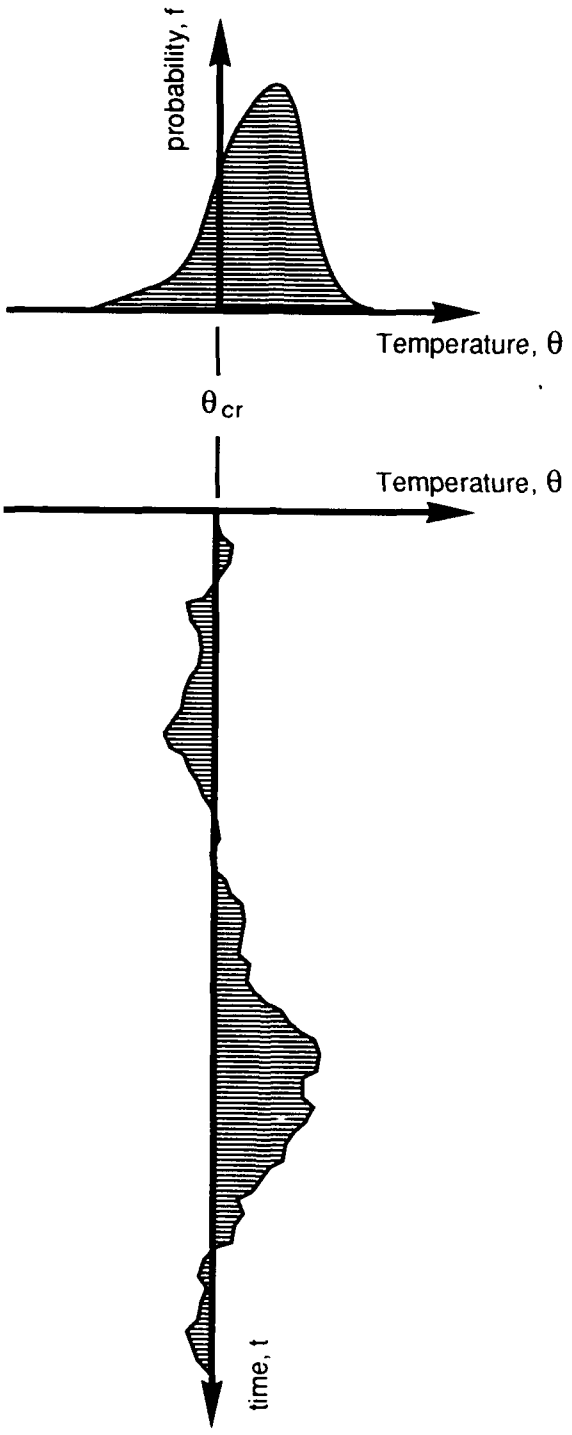

Figure 3. Temperature distribution

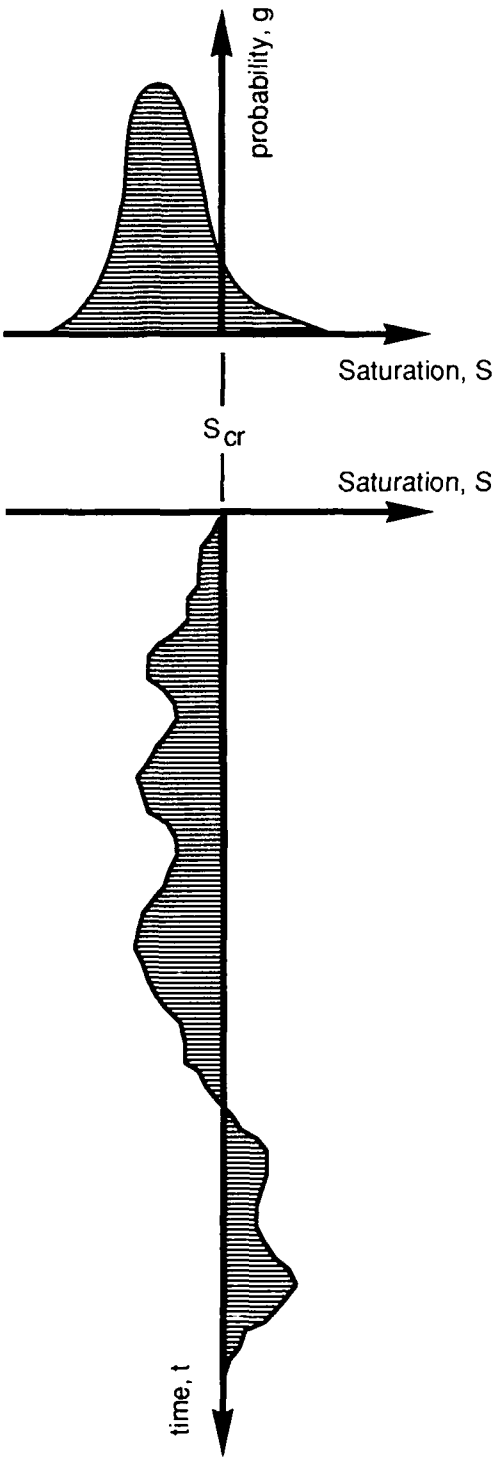

Figure 4. Saturation distribution

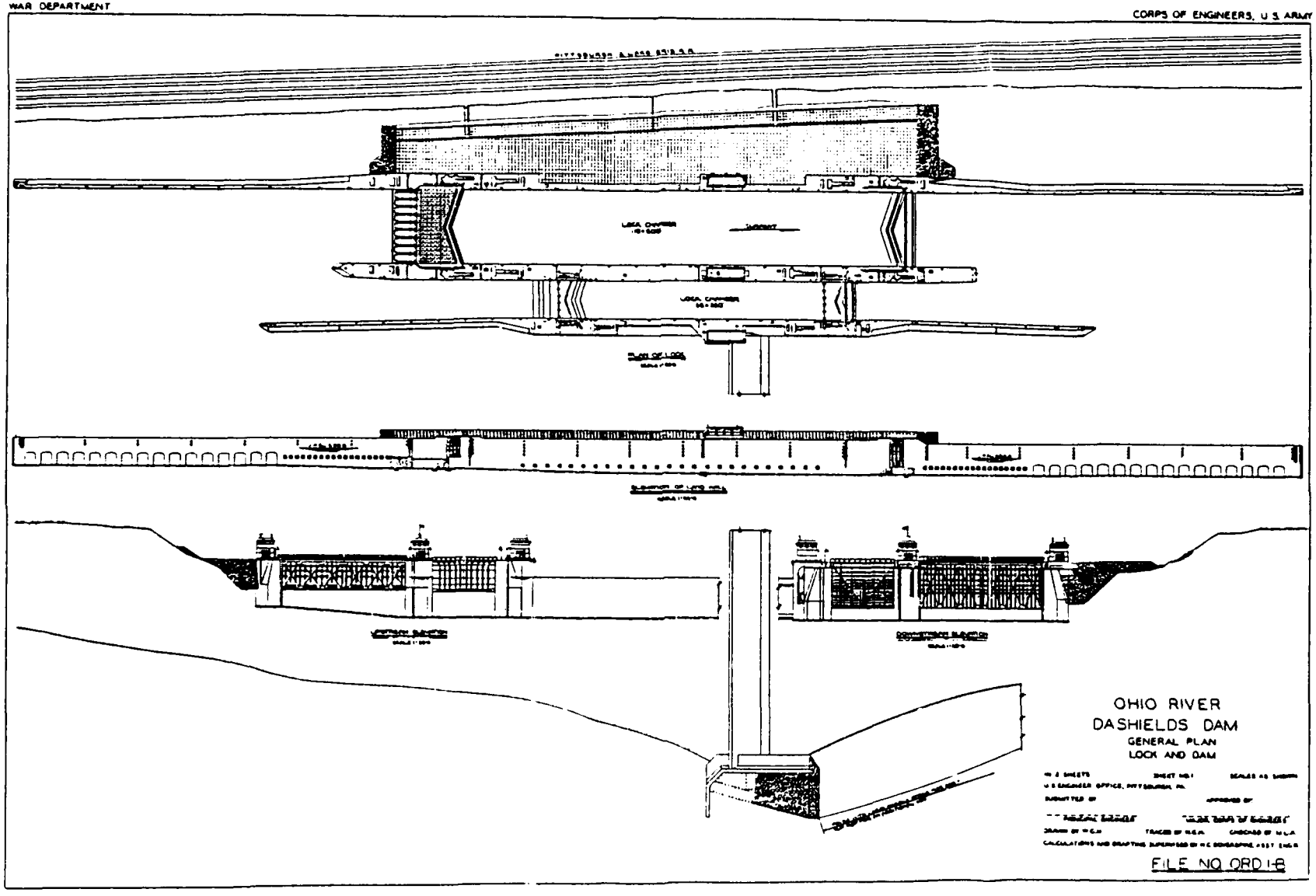

Figure 5. Dashields Lock and Dam

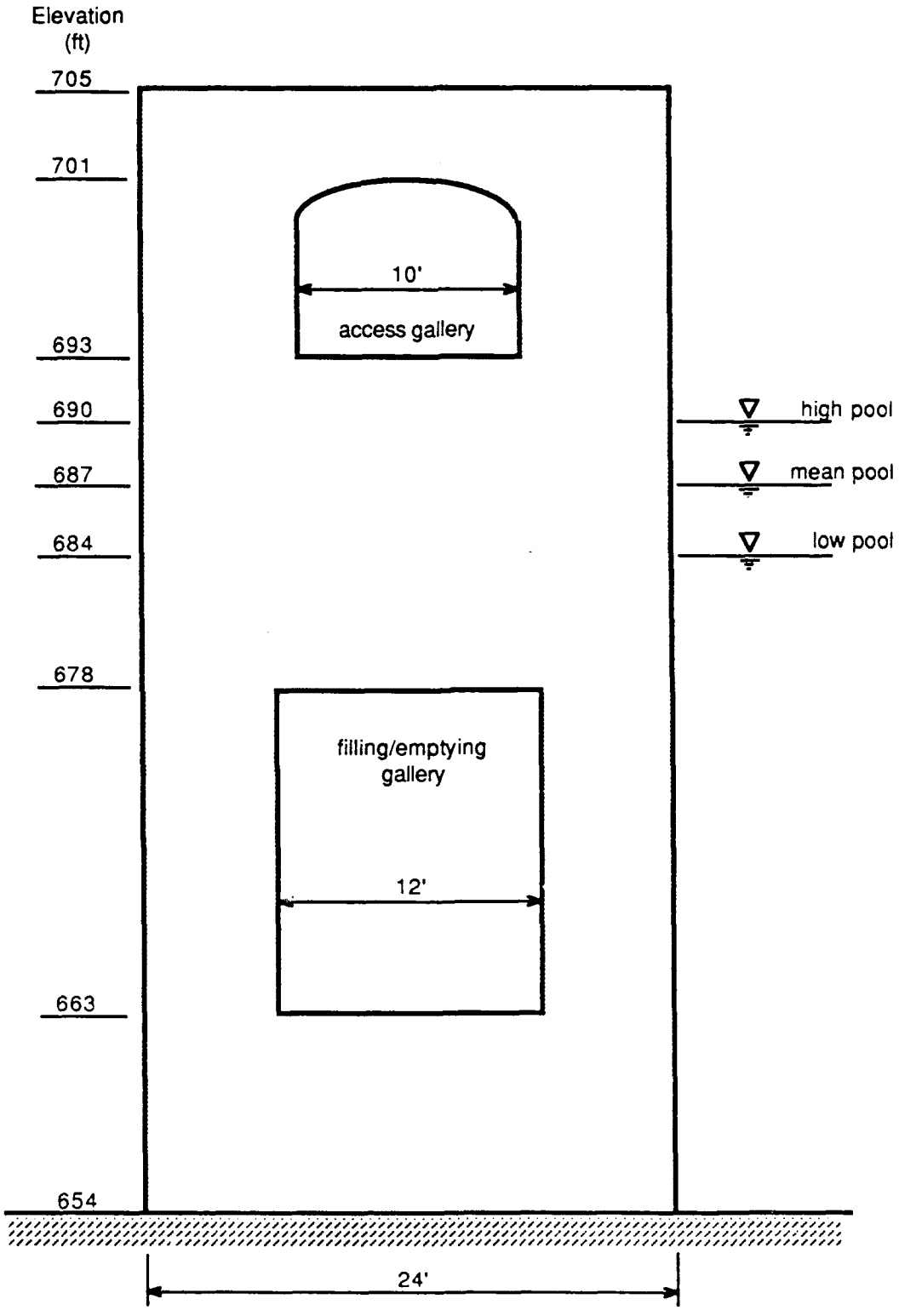

Figure 6. Middle wall at Dashields Lock

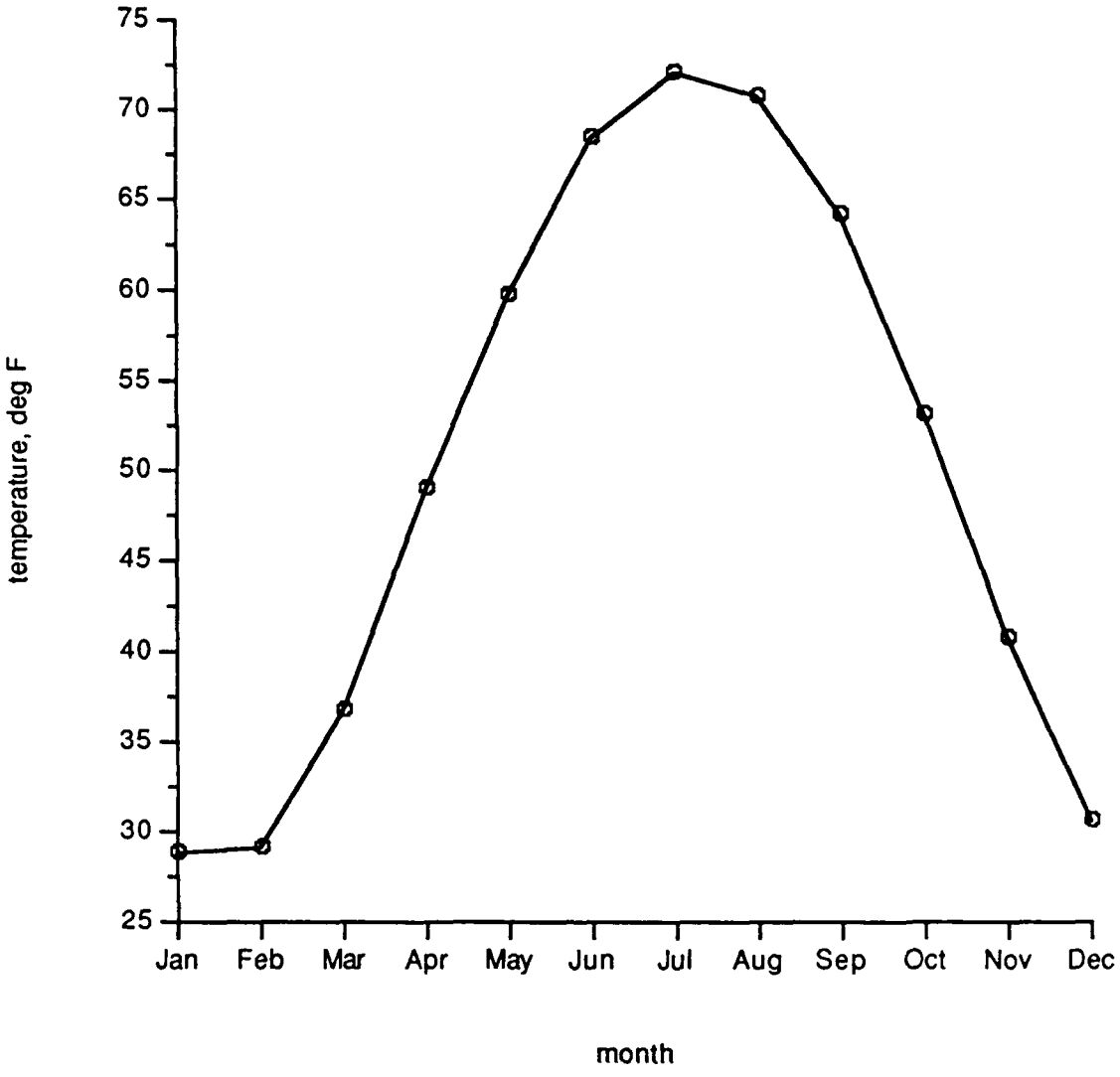

Figure 7. Average monthly air temperatures for Pittsburgh

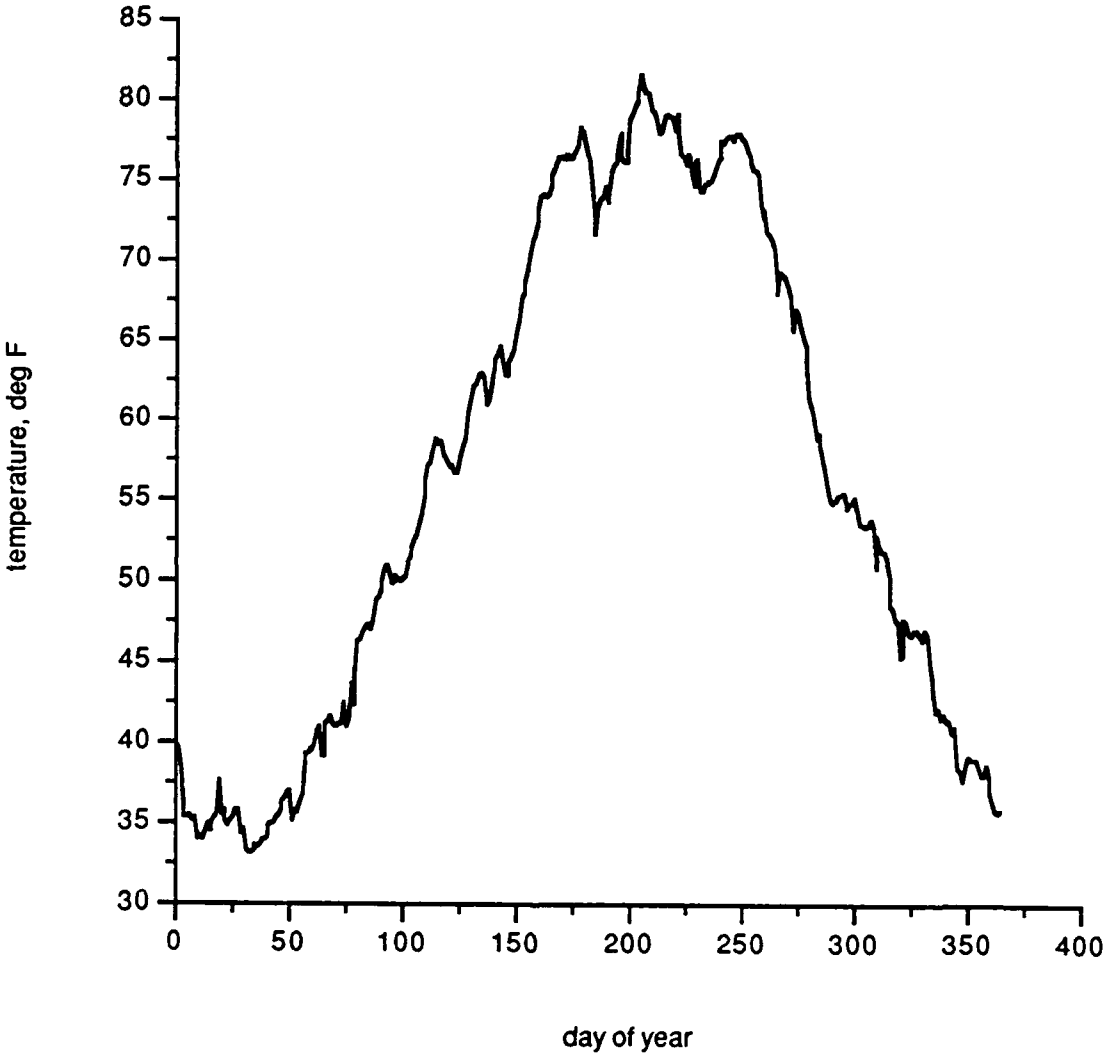

Figure 8. Daily Water temperatures for Dashields Lock

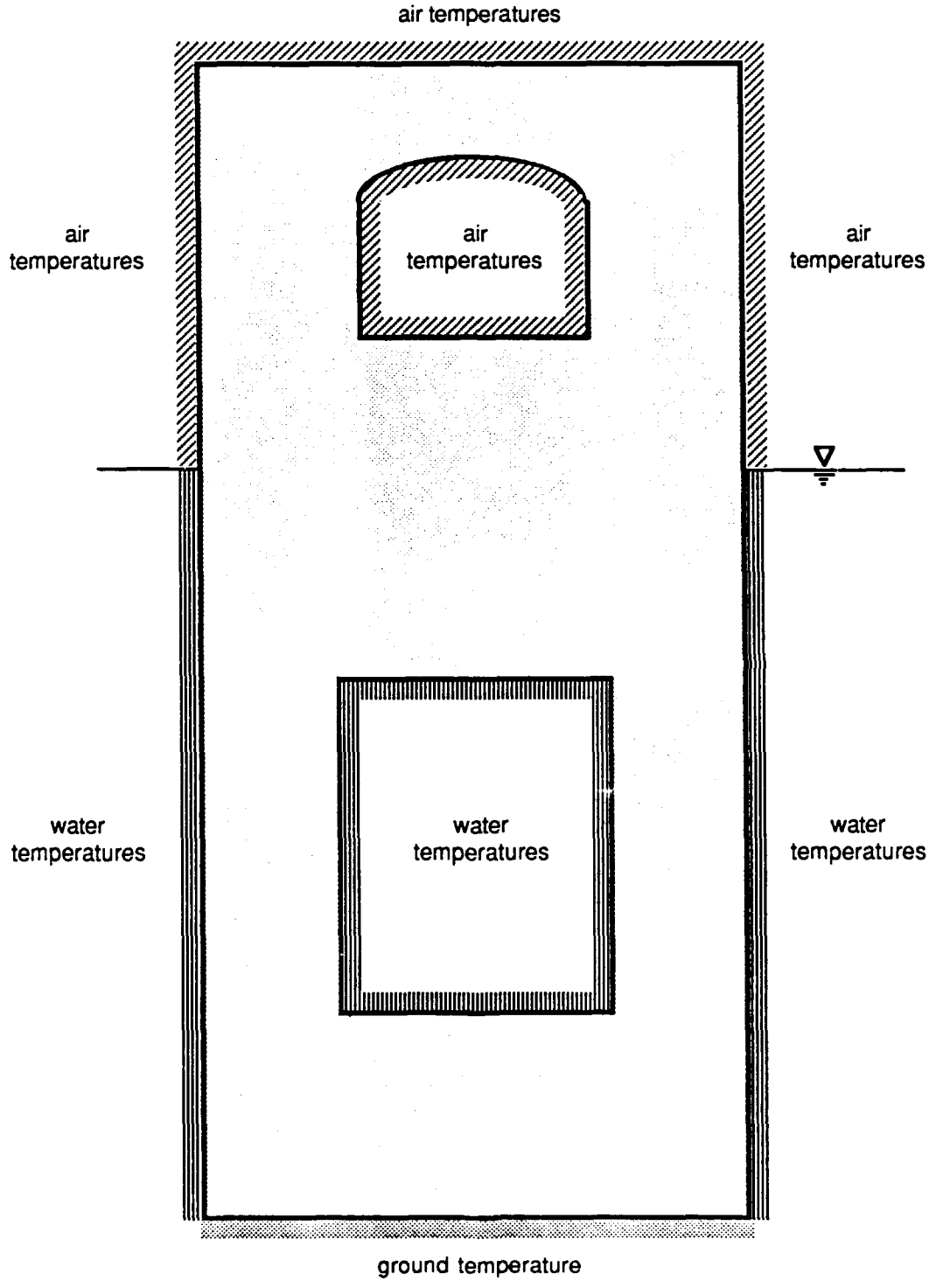

Figure 9. Temperature boundary conditions for middle wall

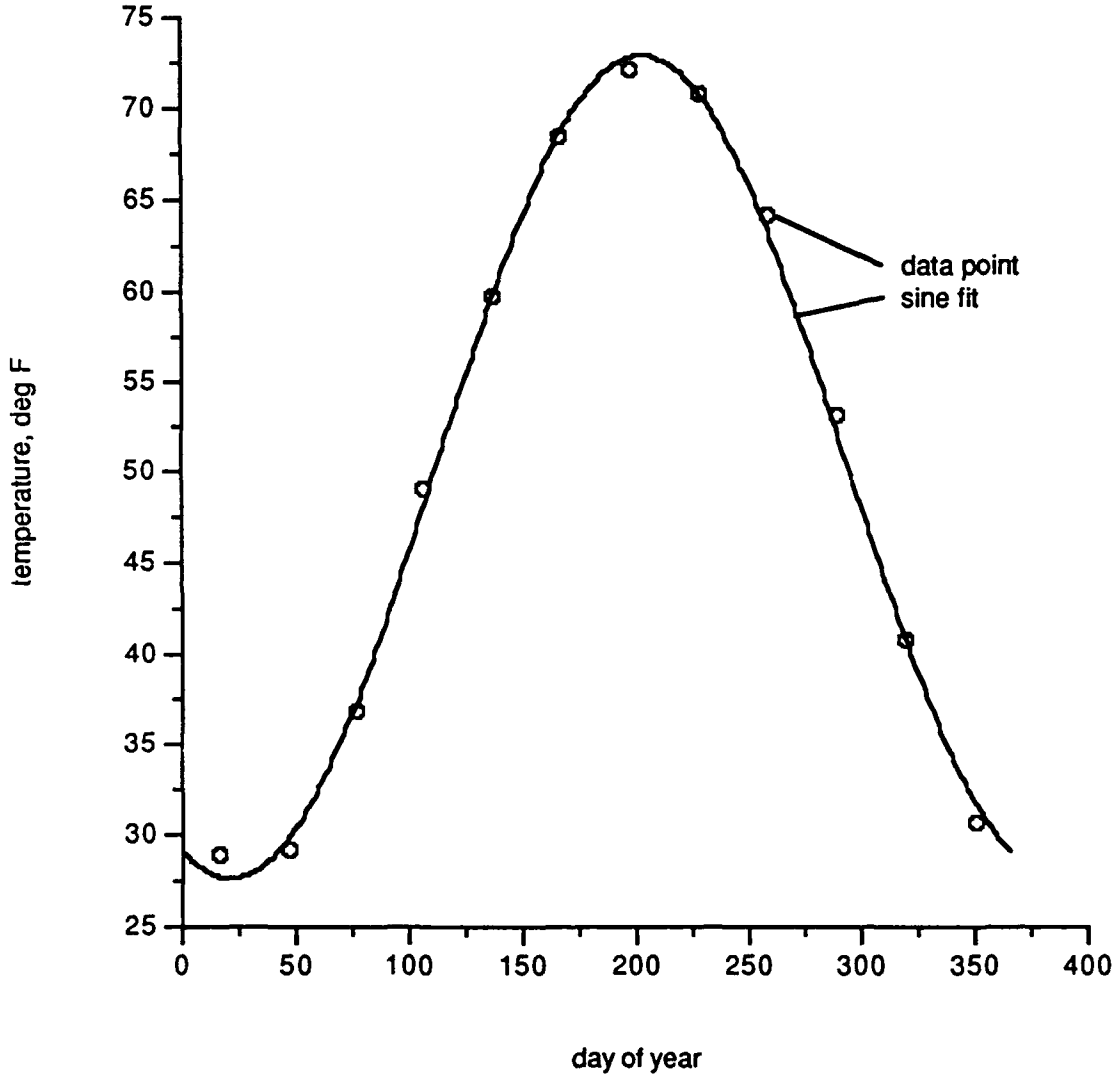

Figure 10. Sinusoidal curve fit to air temperature data

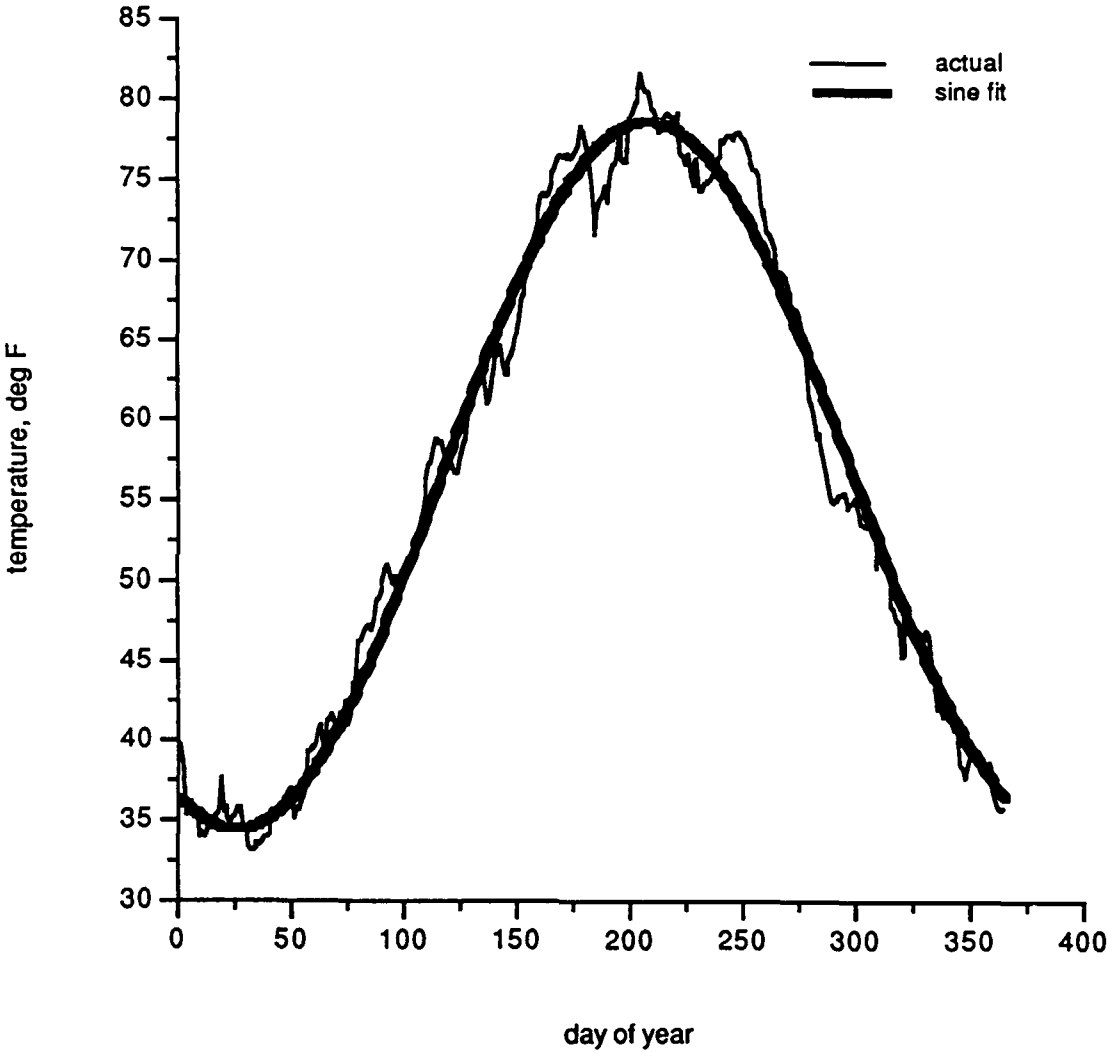

Figure 11. Sinusoidal curve fit to water temperature data

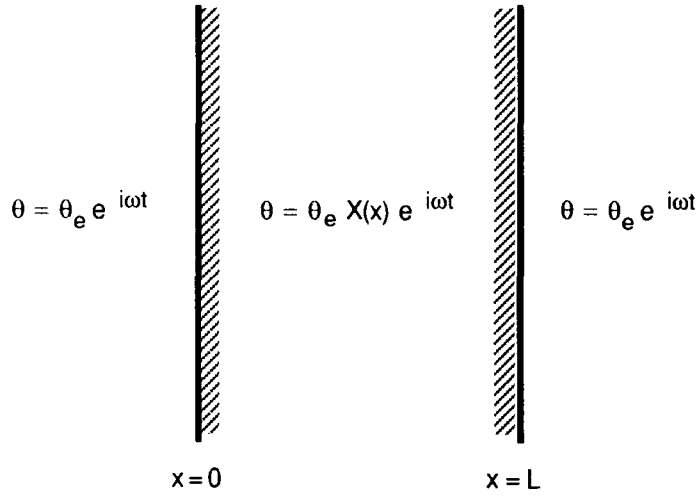

$$X(x') = \frac{\cosh kx'(1+i)}{\cosh kL'(1+i)}$$

$$k^2 = \omega/2h^2 \qquad \omega = 2\pi/365$$

$$x' = x - L/2 \qquad L' = L/2$$

$$\text{temperature attenuation} = |X(x)| = \sqrt{\frac{\cosh k(2x-L) + \cos k(2x-L)}{\cosh kL + \cos kL}}$$

where: h^2 = thermal diffusivity

θ_e = external temperature

ω = temperature frequency

L = wall thickness

Figure 12. One-dimensional thermal analysis model of wall

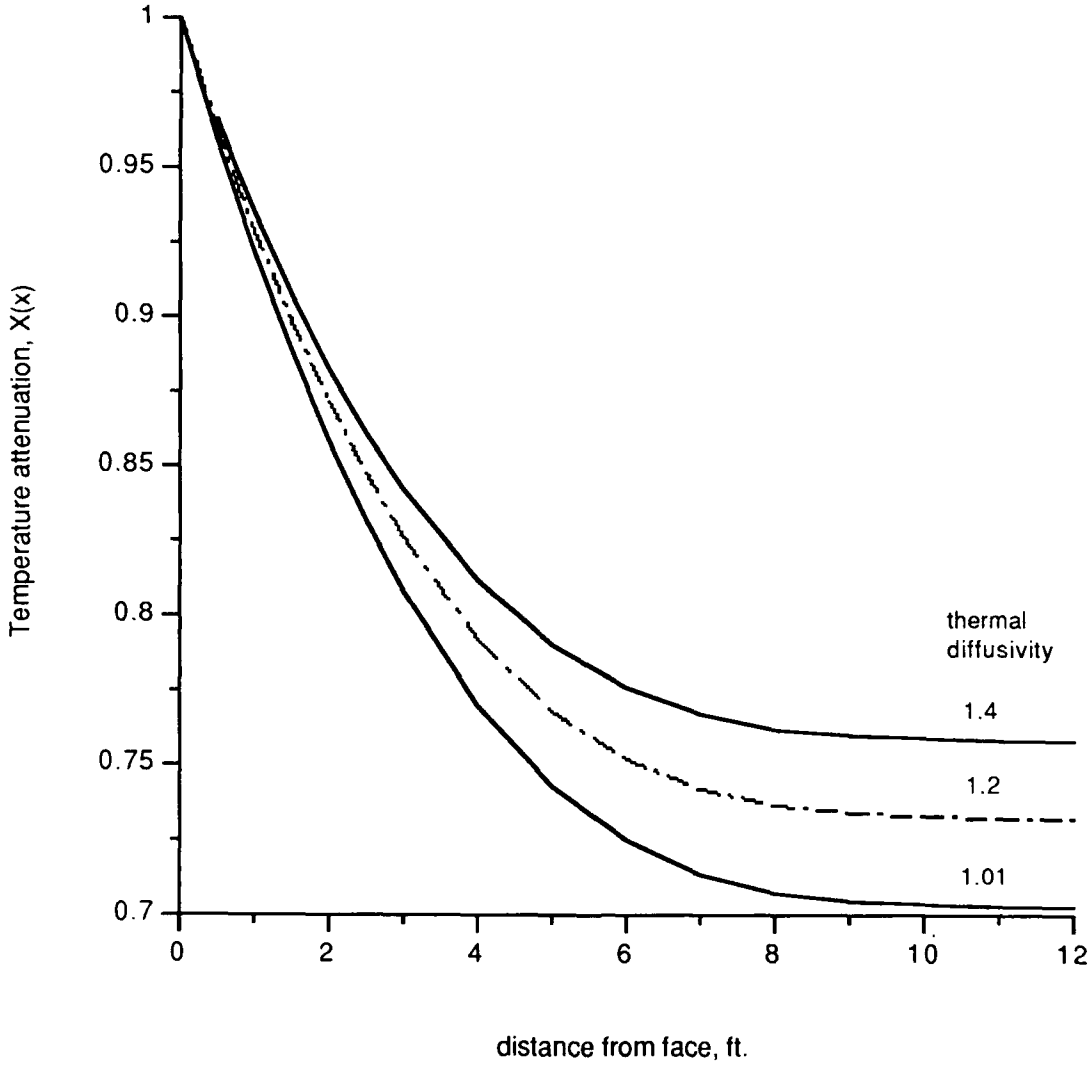

Figure 13. Attenuation of temperature with distance and thermal diffusivity

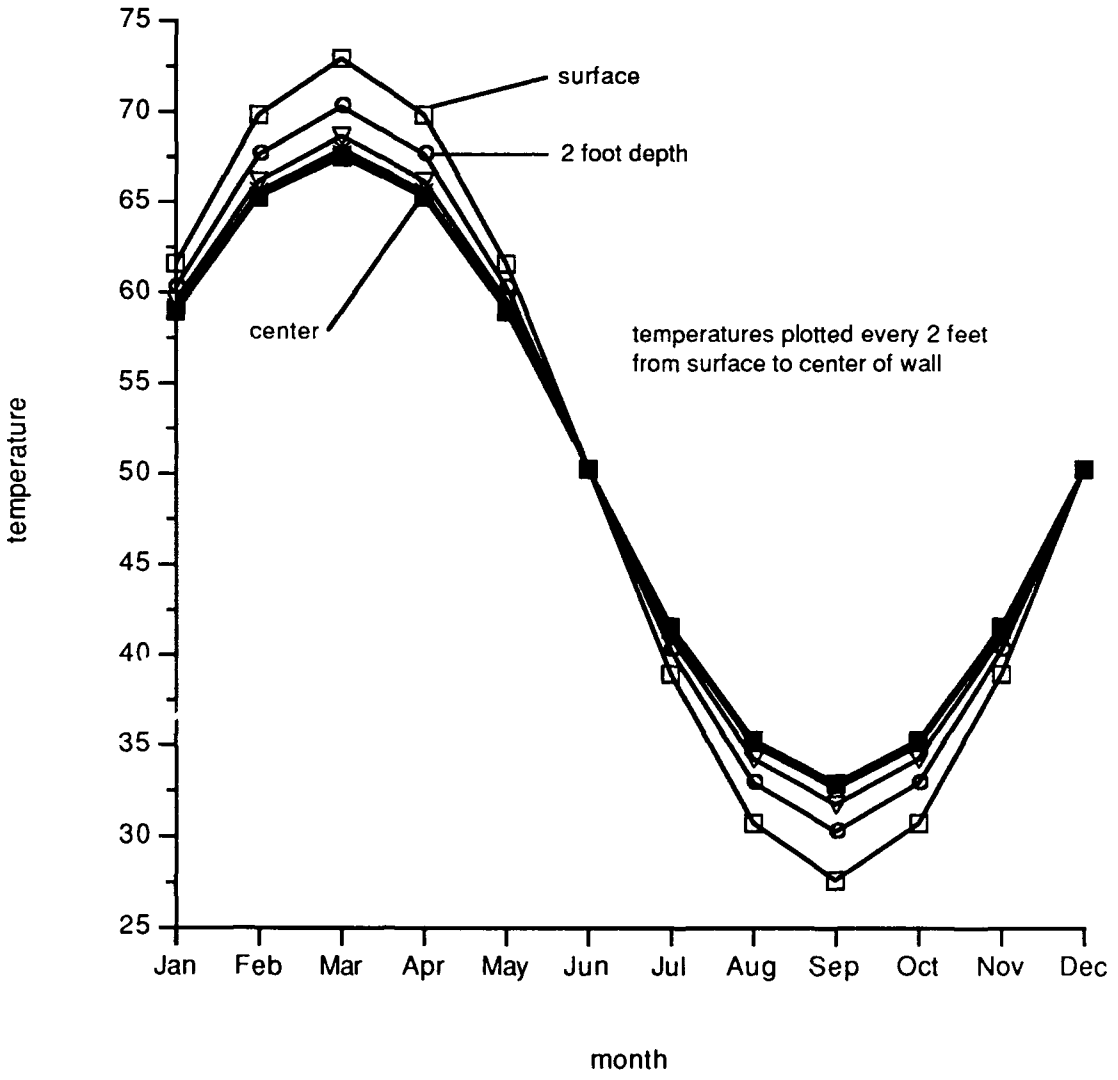

Figure 14. Annual temperature cycles at various depths (above waterline)

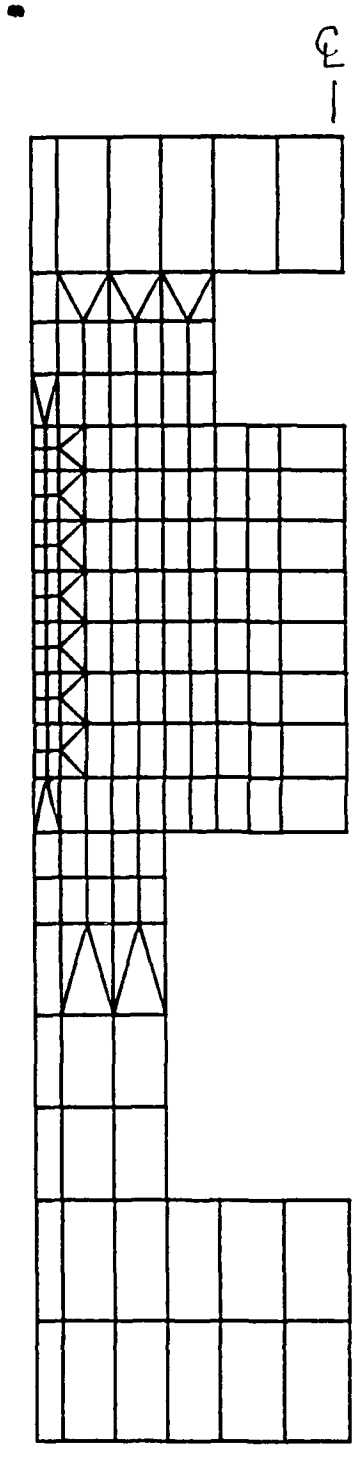

Figure 15. Finite-element thermal analysis model of middle wall

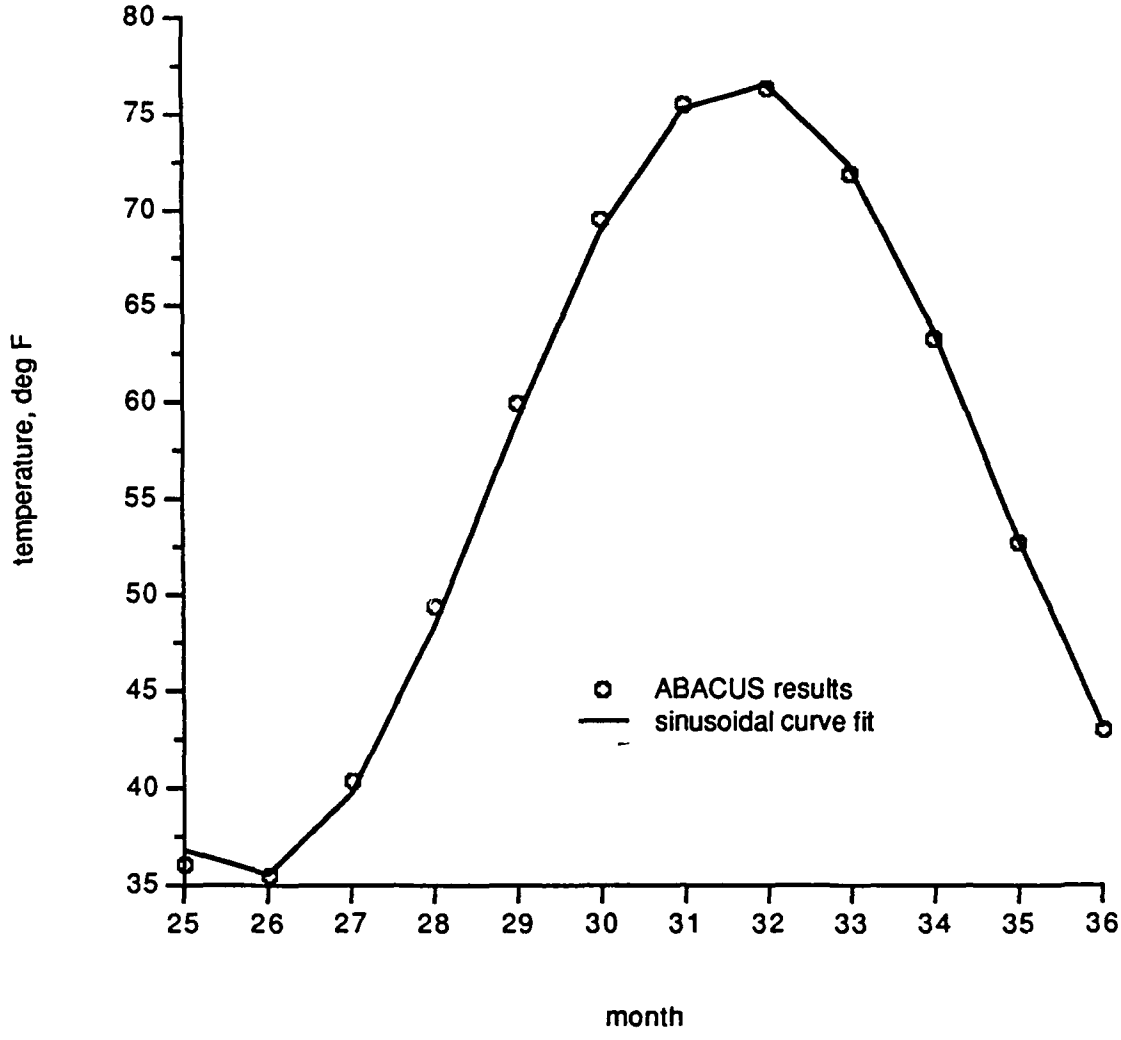

mean = 56.04°F amplitude = 20.74°F

Figure 16. Sinusoidal curve fit for node 2118

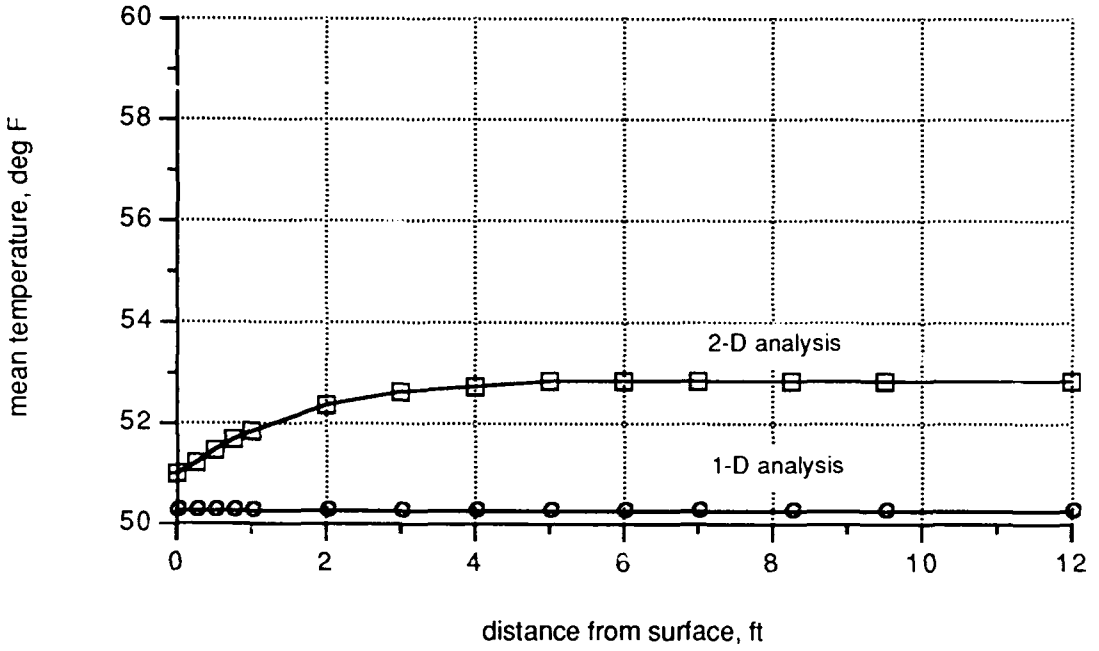

a. Mean temperature

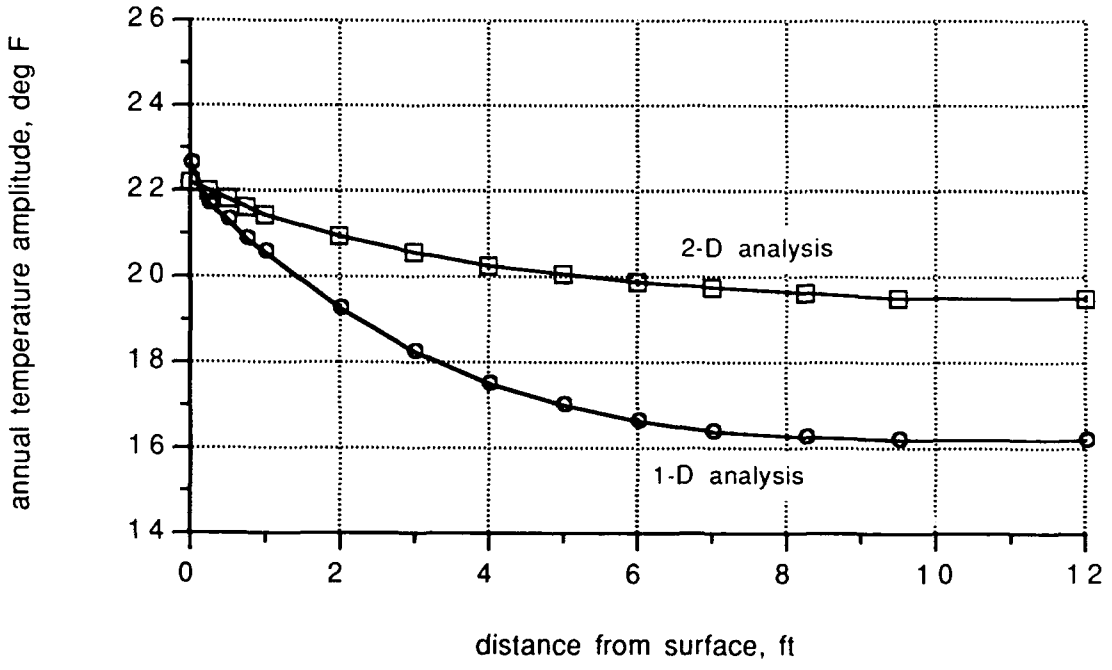

b. Annual amplitude of temperature

Figure 17. Comparison of temperatures from 1- and 2-D analyses (2 feet above waterline)

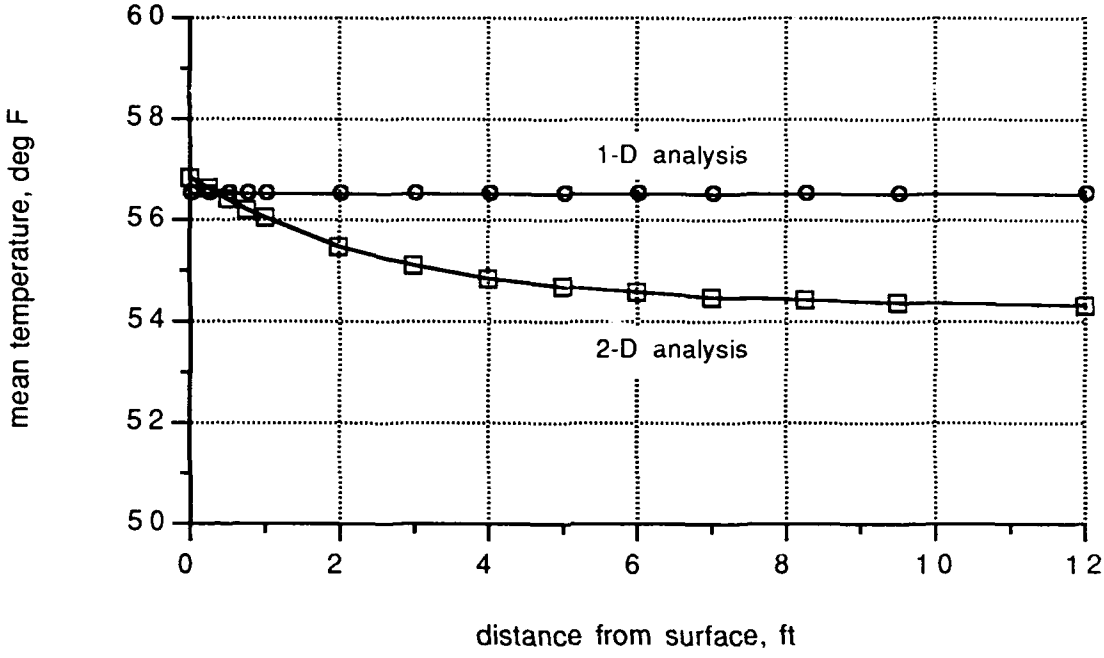

a. Mean temperature

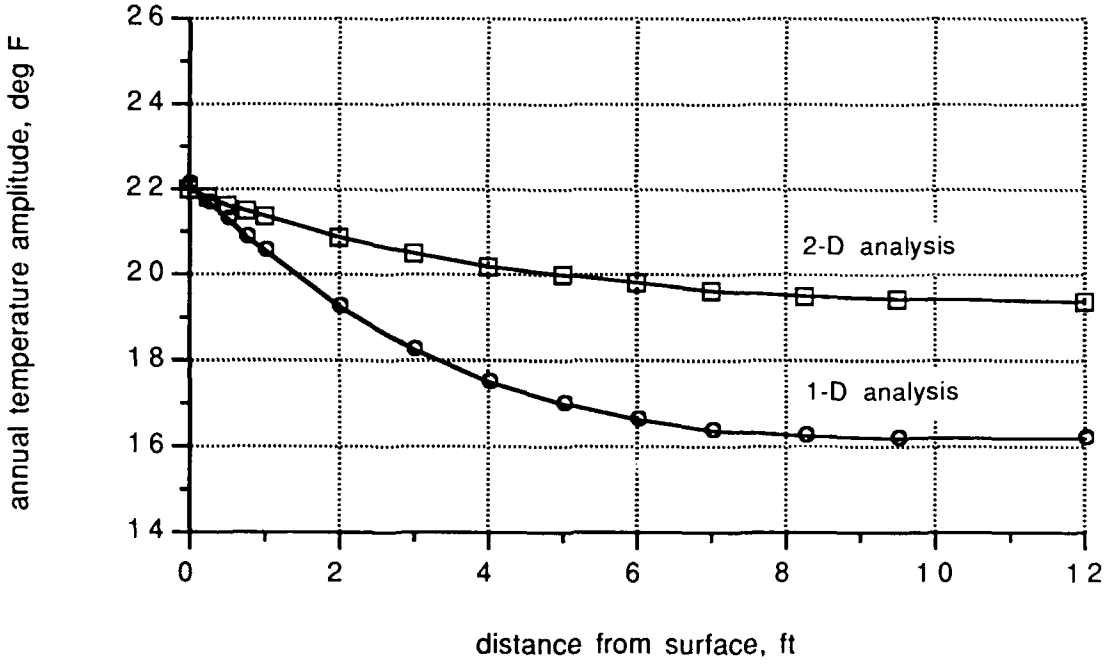

b. Annual amplitude of temperature

Figure 18. Comparison of temperatures from 1- and 2-D analyses (2 feet below waterline)

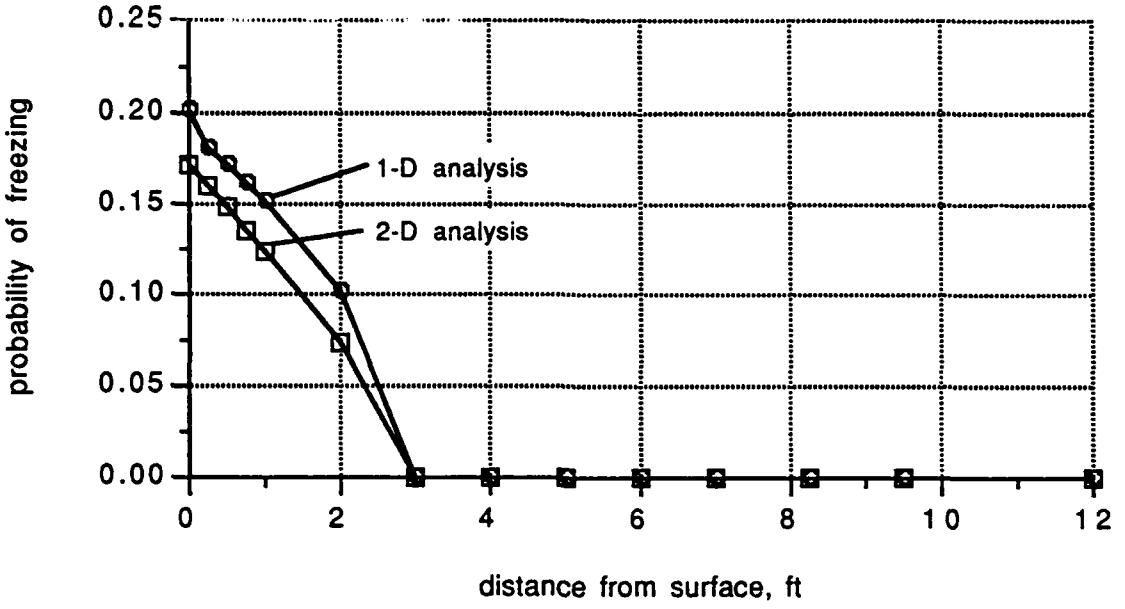

a. Section above waterline

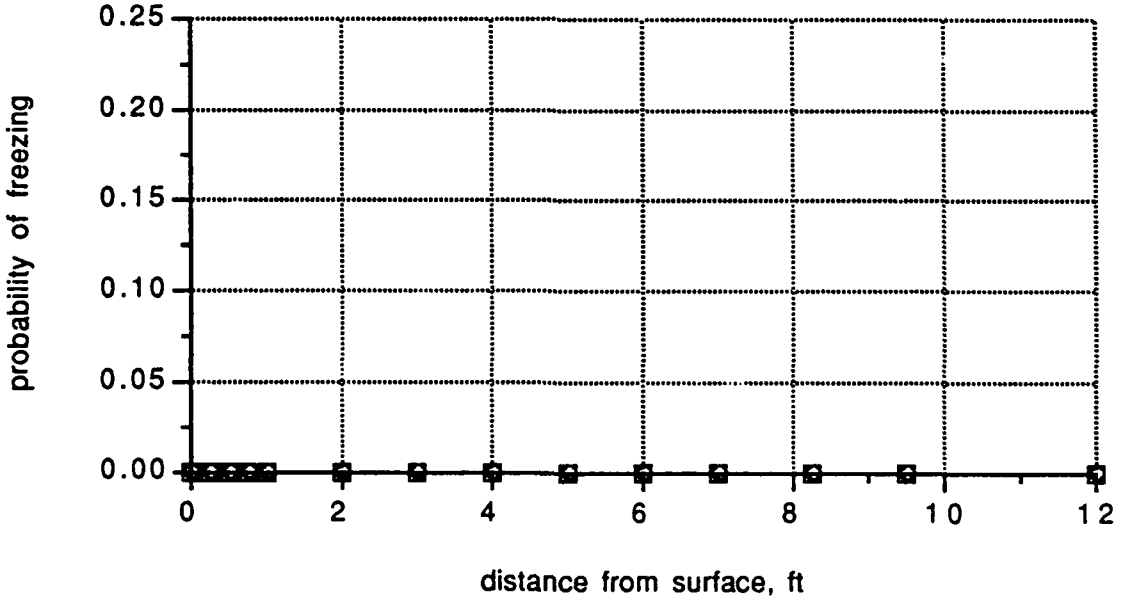

b. Section below waterline

Figure 19. Comparison of probability of freezing for 1- and 2-D analyses

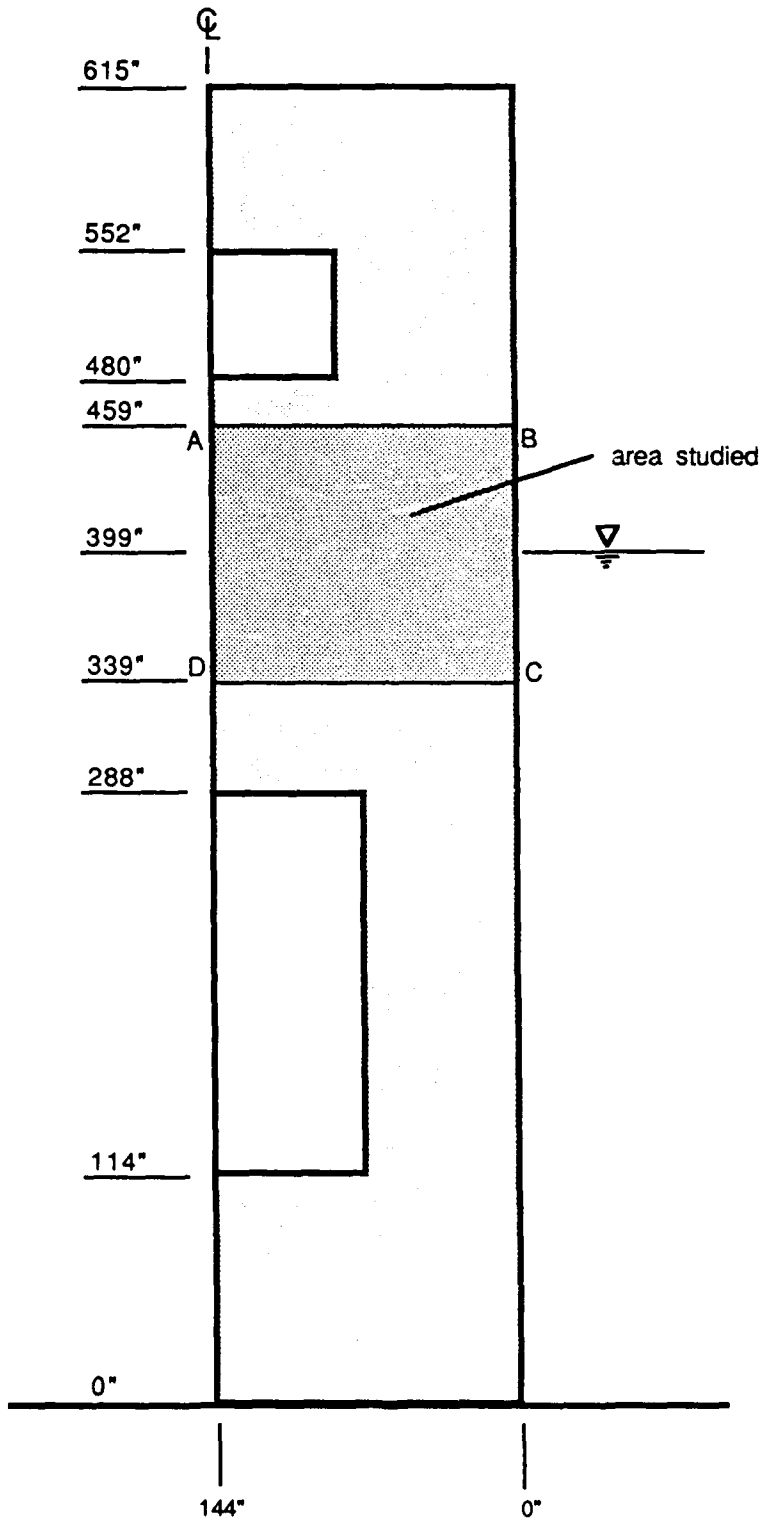

Figure 20. Area of middle wall studied in more detail

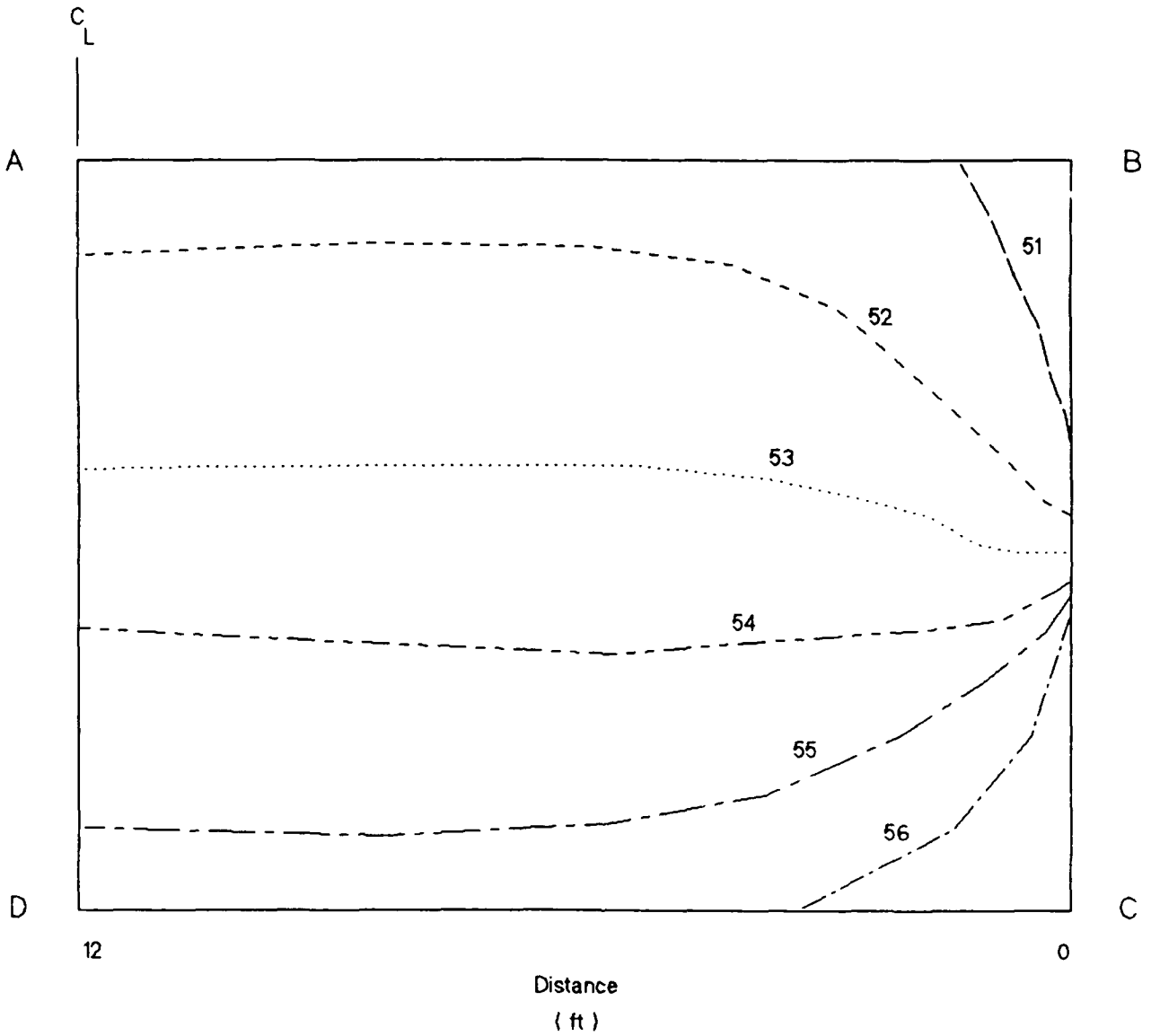

Figure 21. Mean temperatures (°F) in middle wall.
See Figure 20 for orientation of this section

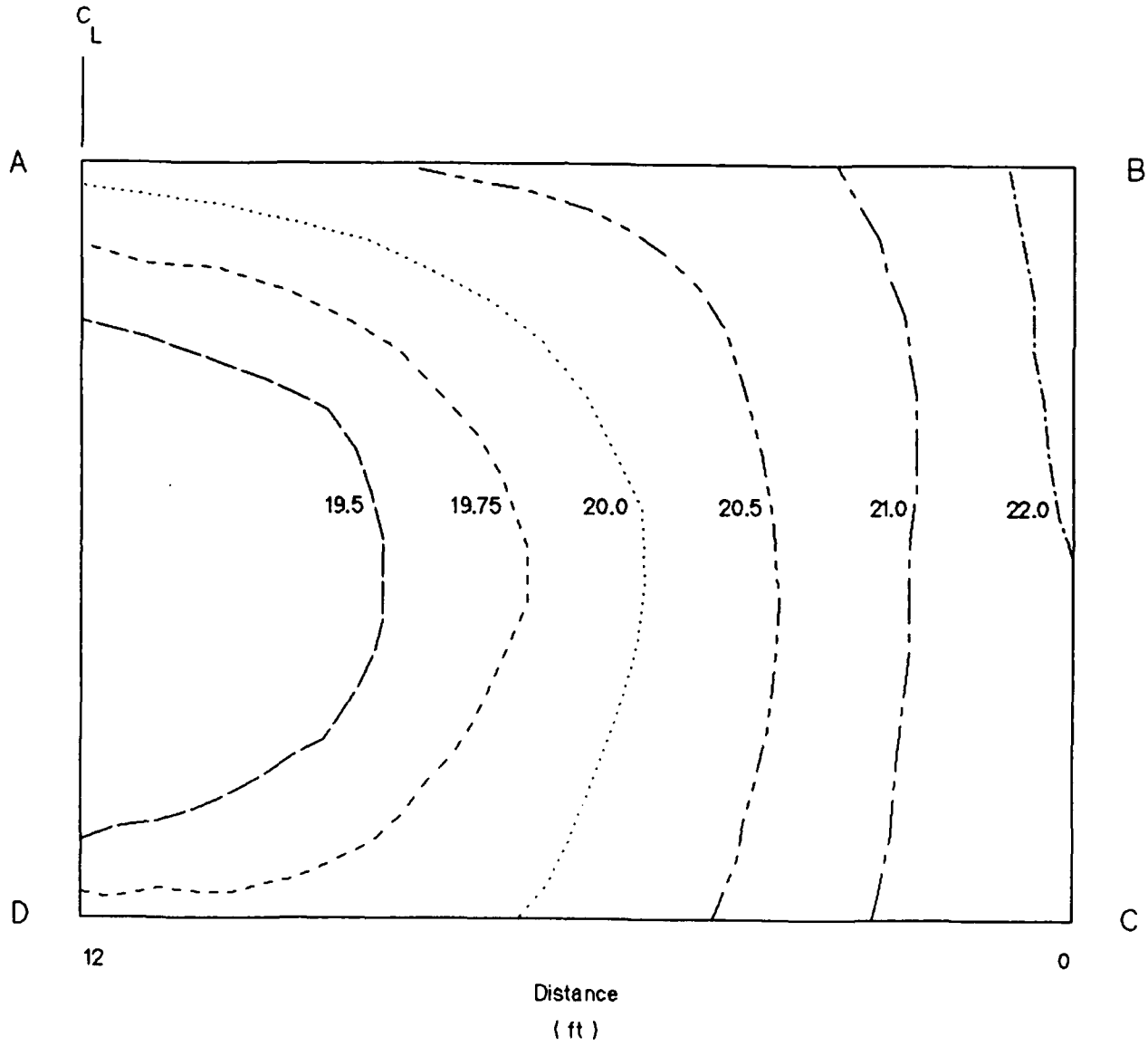

Figure 22. Mean temperature (°F) amplitudes in middle wall.
See Figure 20 for orientation of this section

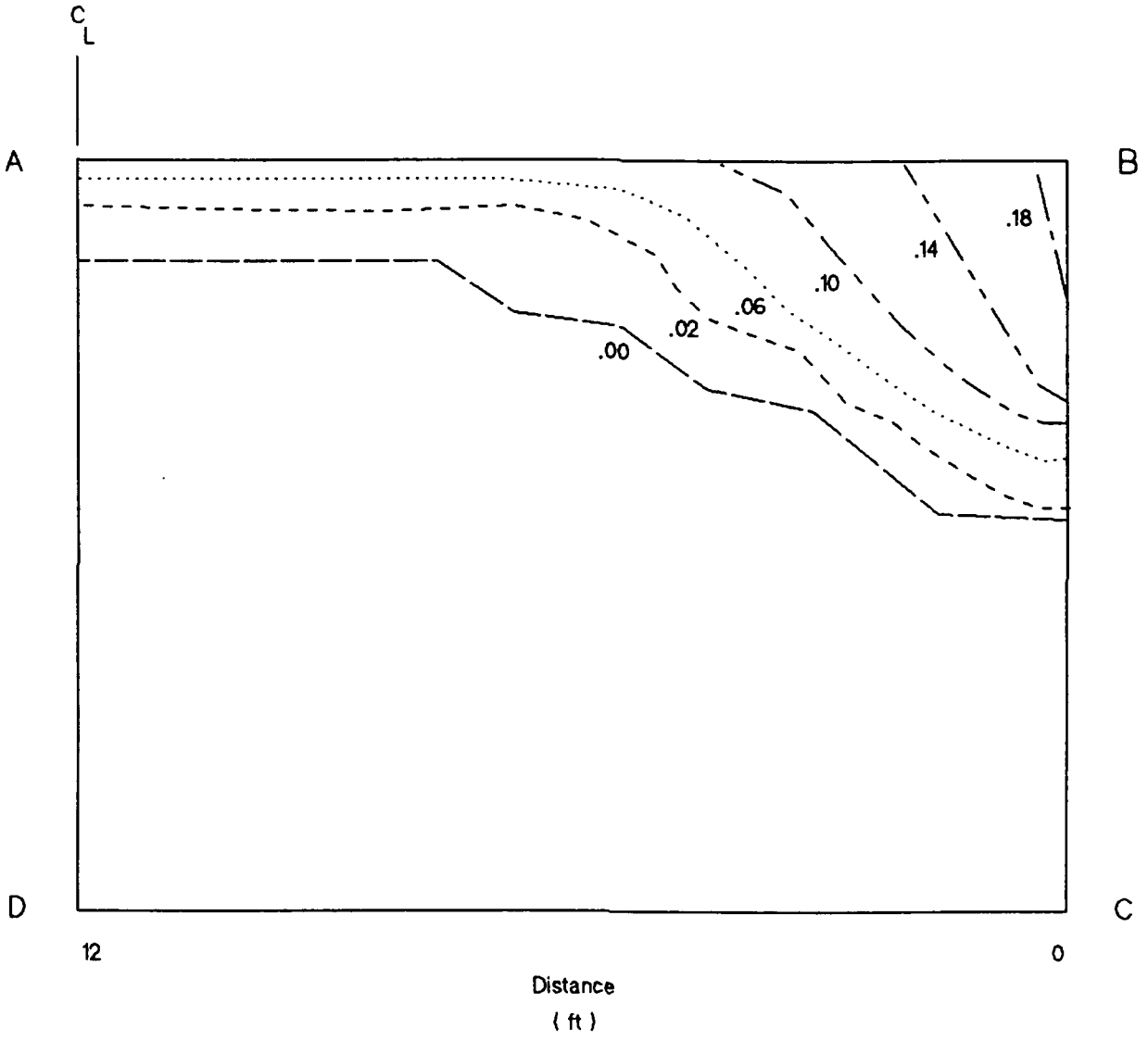

Figure 23. Probability of freezing in middle wall.
See Figure 20 for orientation of this section

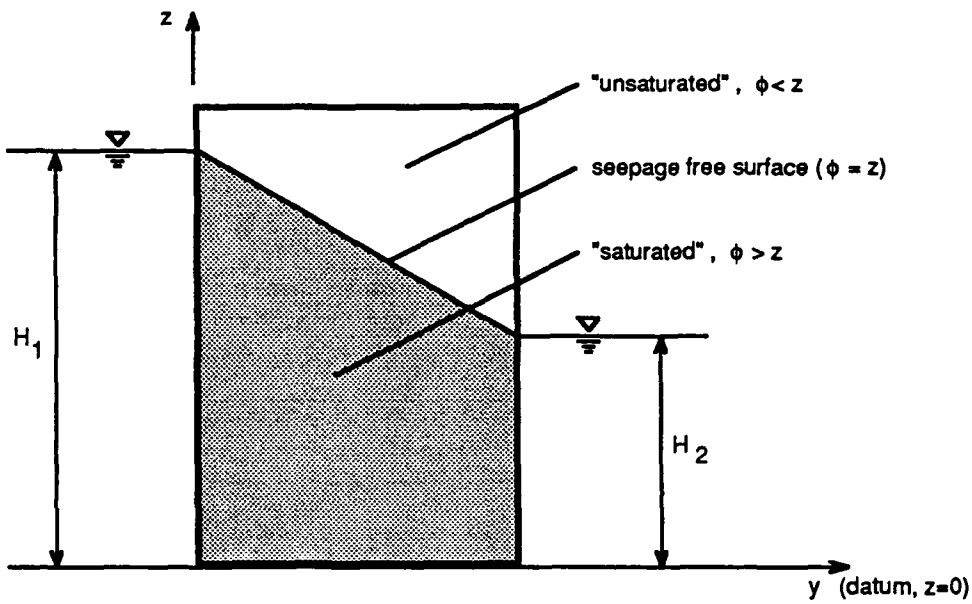

ϕ = total fluid head or potential

$= z + p/\gamma$

where:
p = fluid pressure
γ = fluid unit weight
z = elevation above datum

Figure 24. Seepage model of middle wall

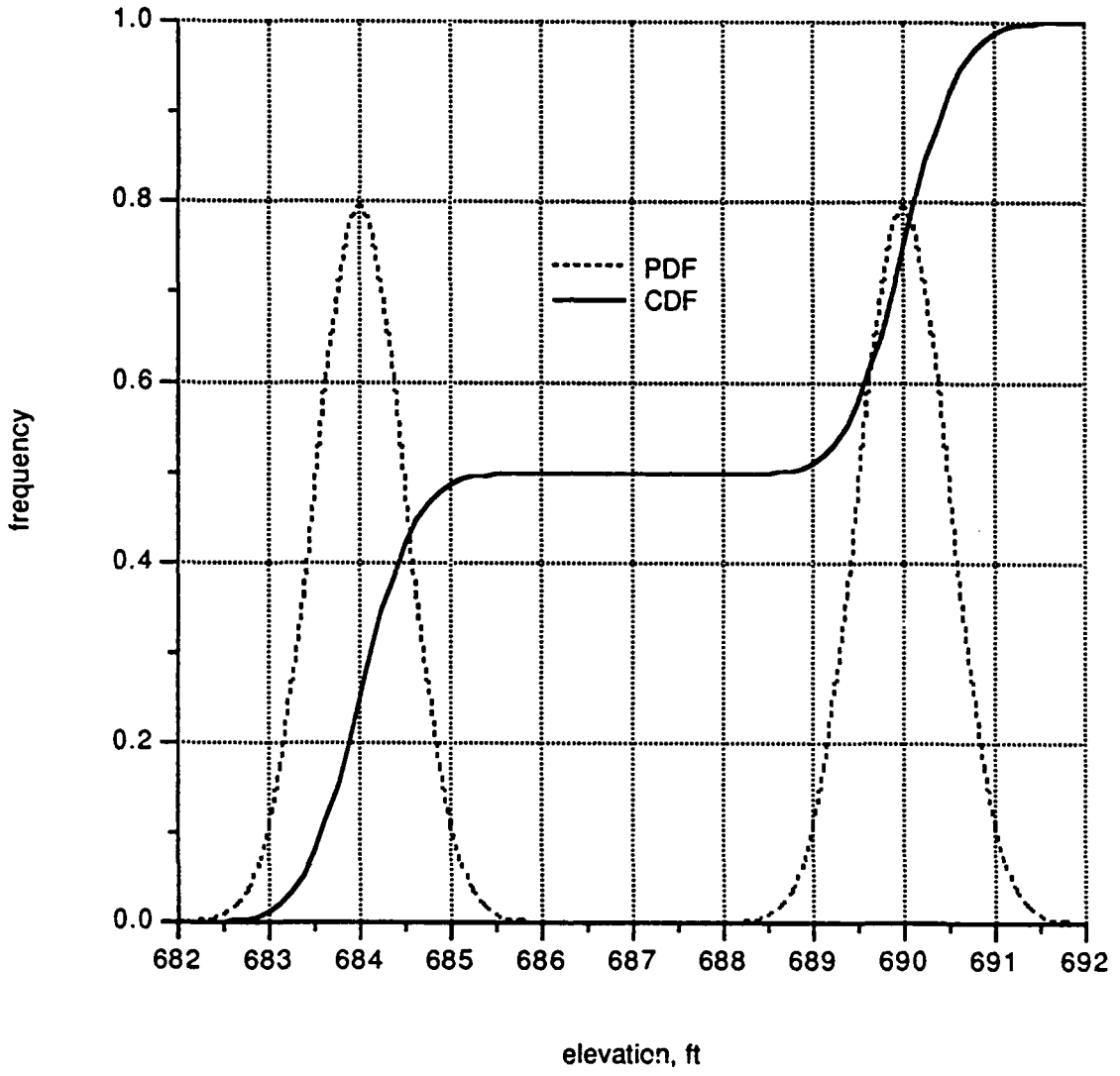

Figure 25. Distribution of lock pool elevations

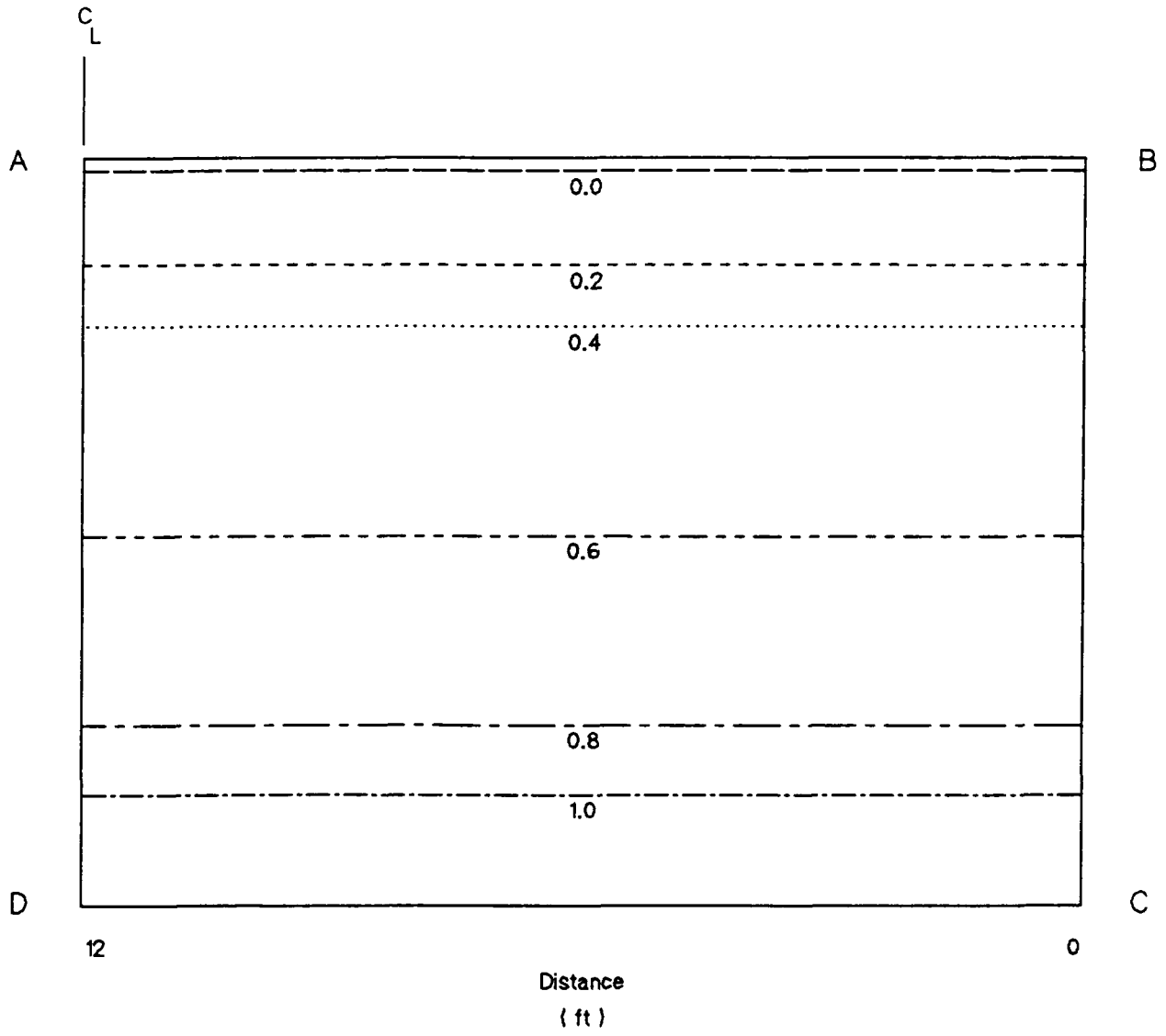

Figure 26. Probability of critical saturation in middle wall.
See Figure 20 for orientation of this section

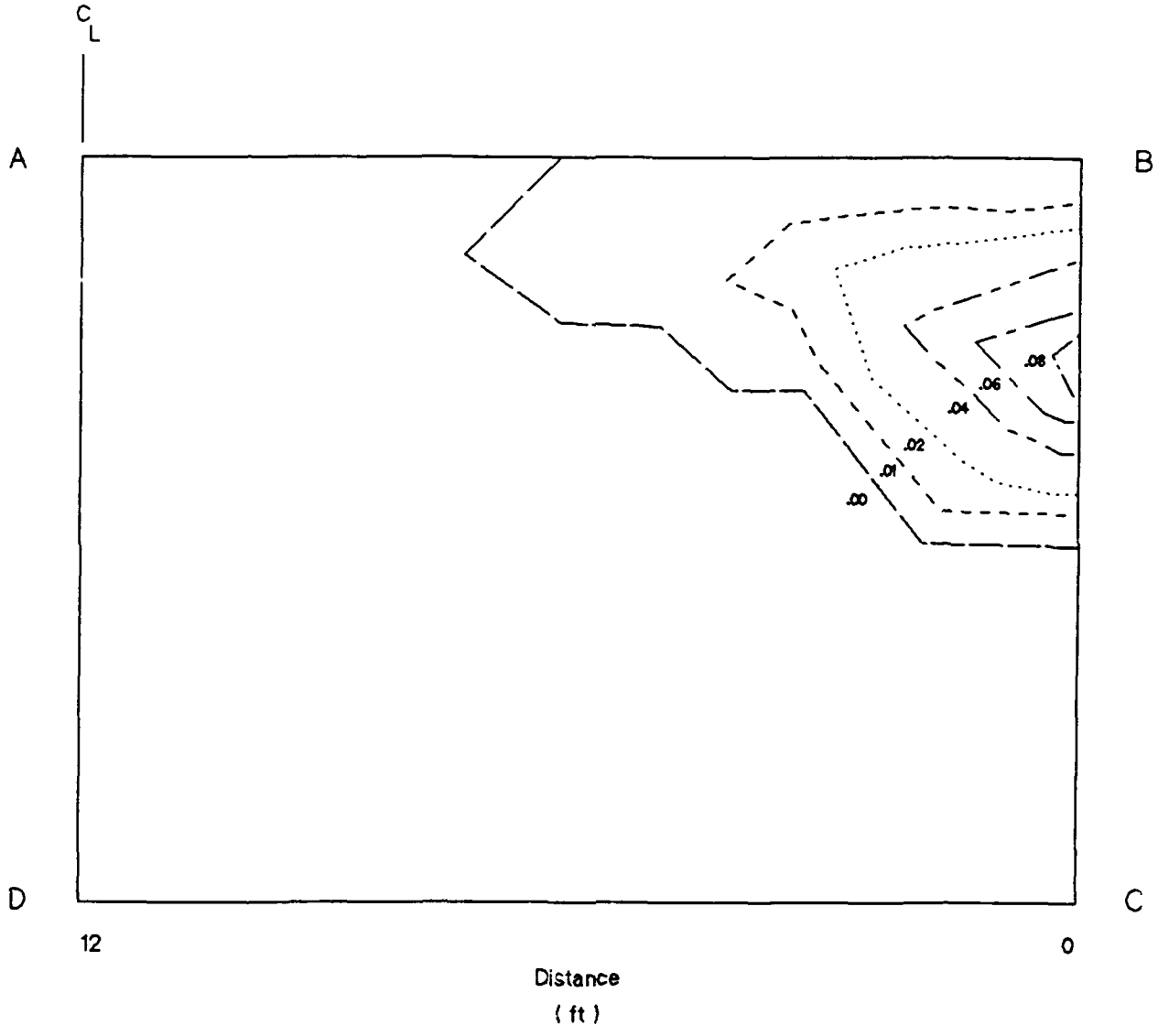

Figure 27. Annual probability of damage for middle wall at Dashields Lock. See Figure 20 for orientation of this section

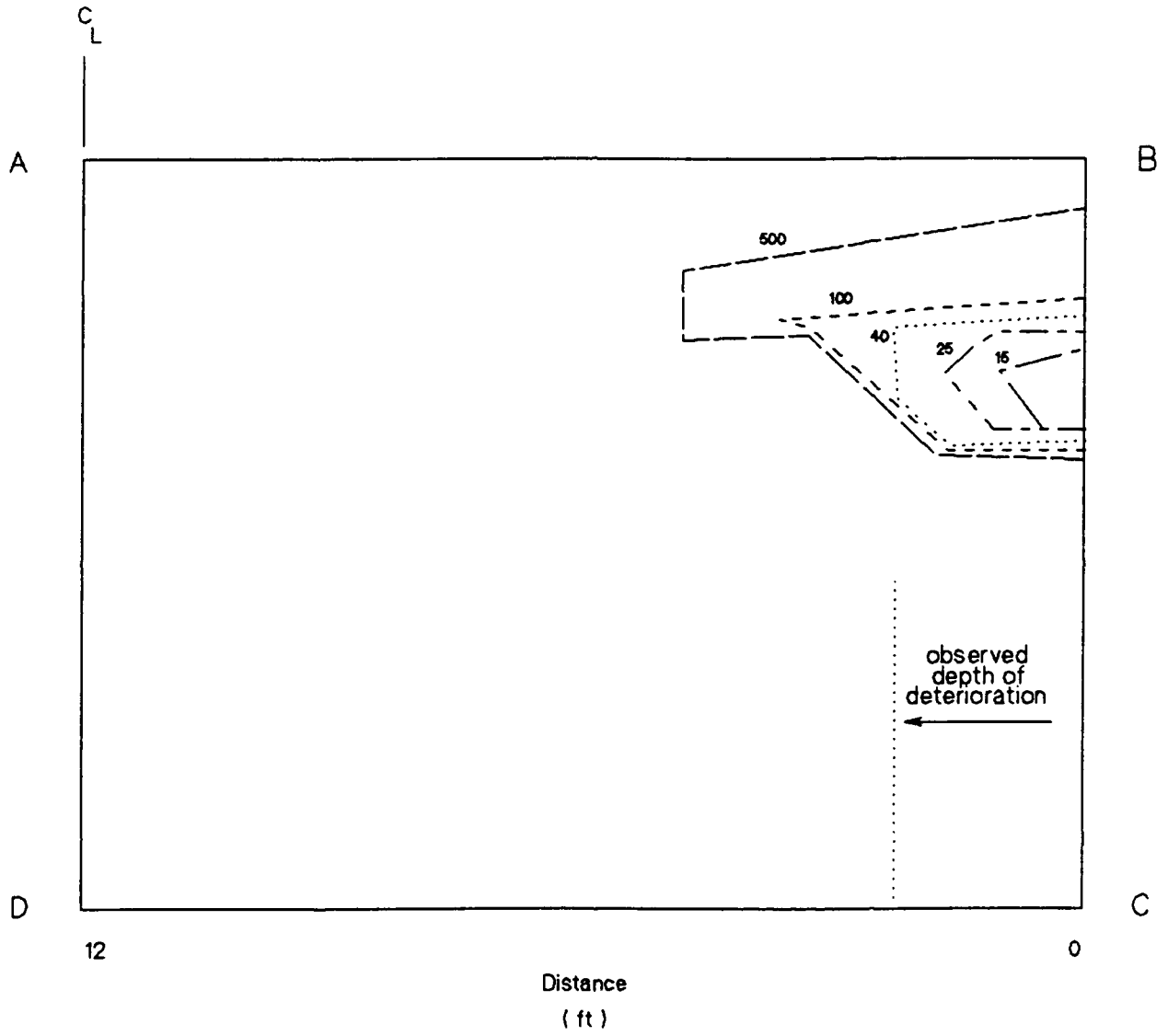

Figure 28. Service life (yrs) prediction for middle wall at Dashields Lock. See Figure 20 for orientation of this section

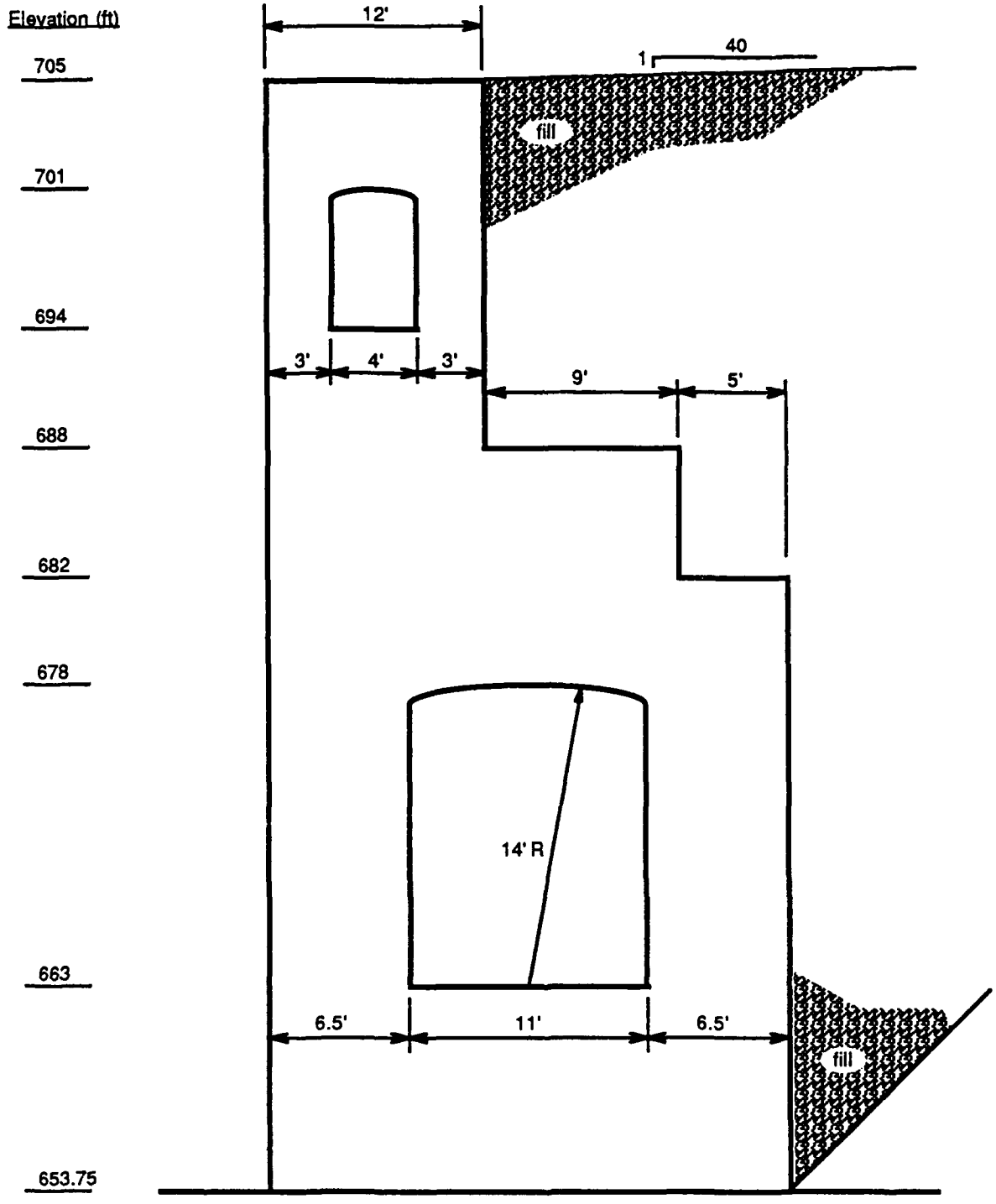

Figure 29. Section through land wall at Dashields Lock

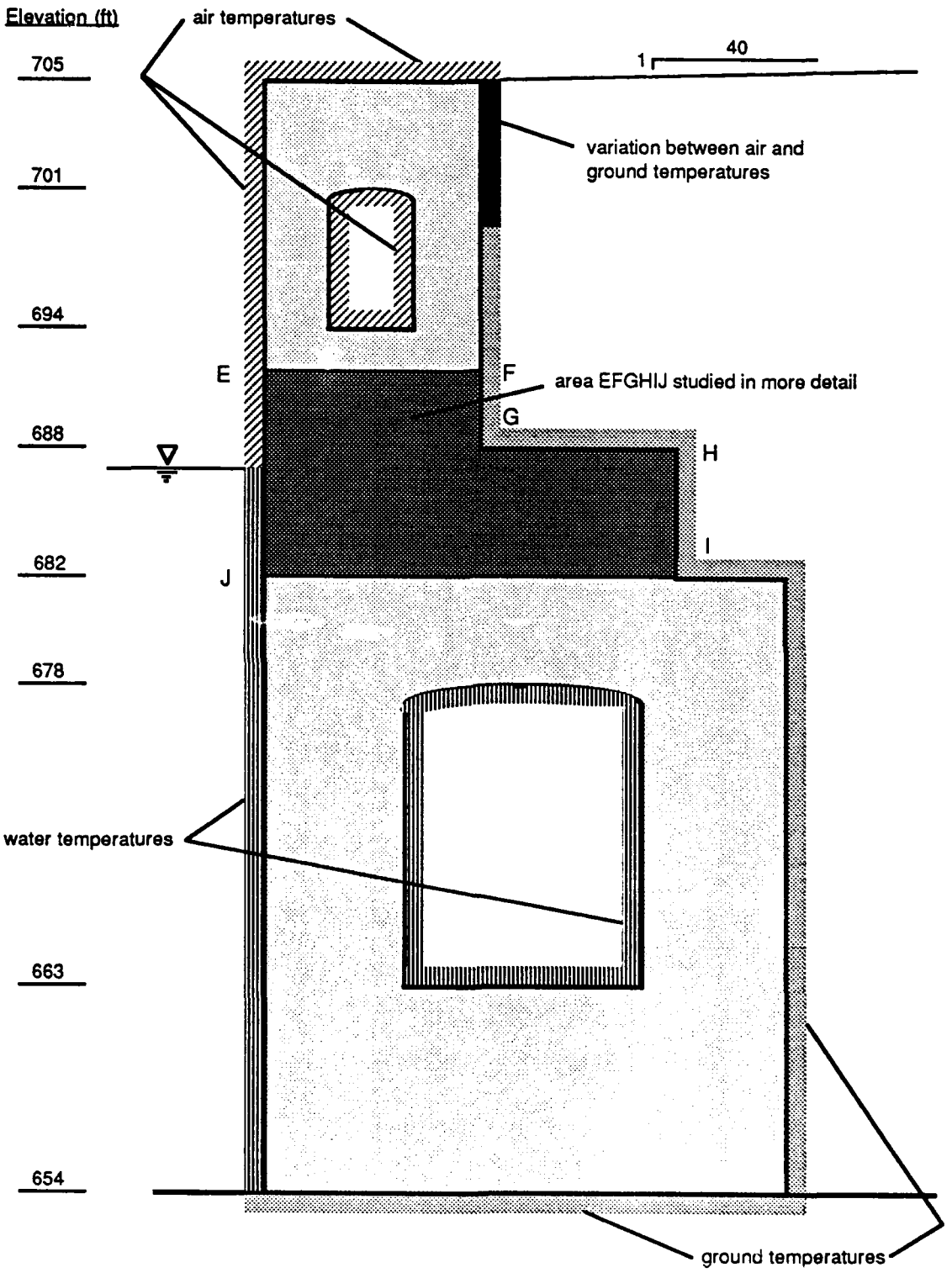

Figure 30. Temperature boundary conditions for land wall

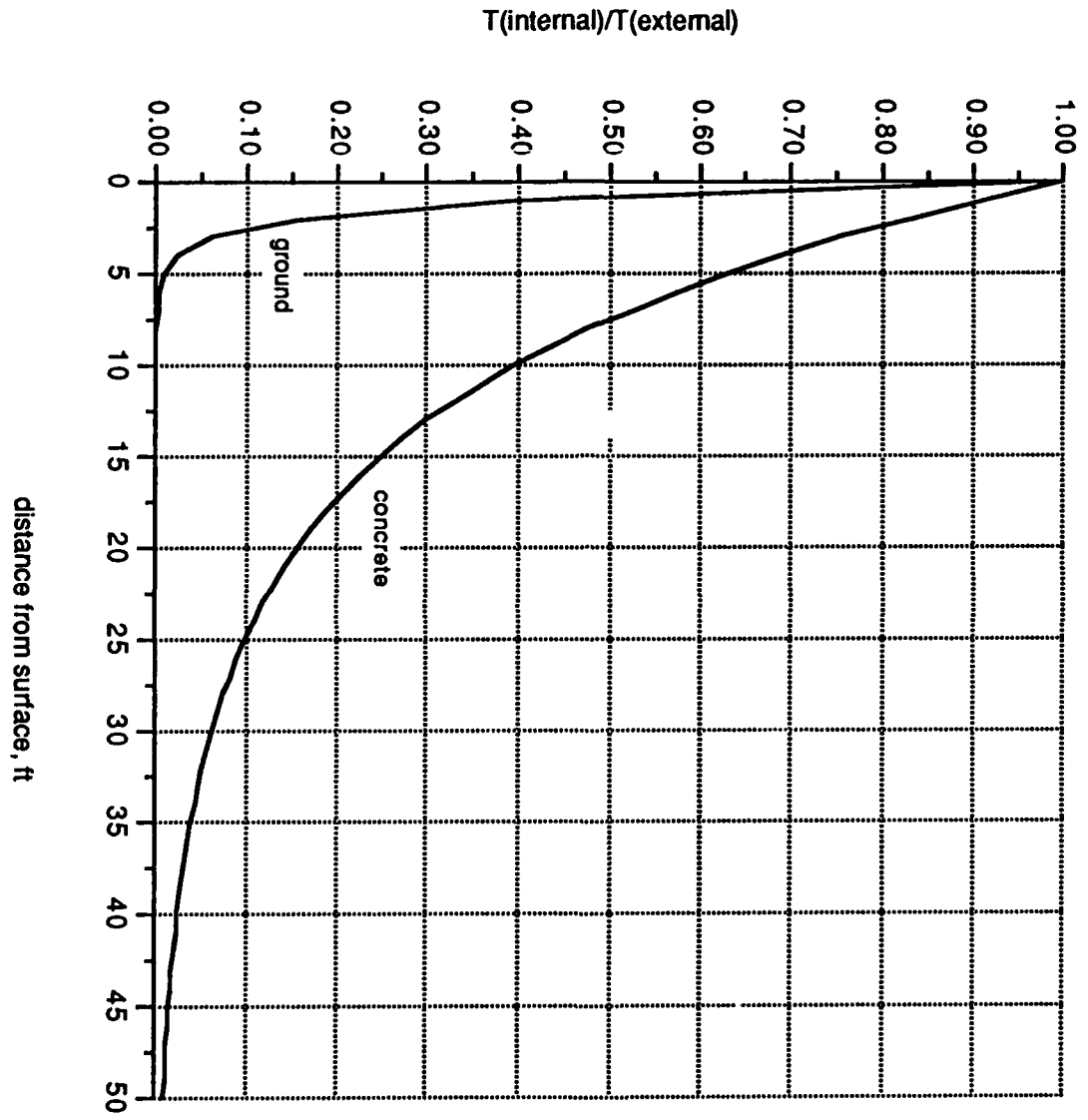

Figure 31. Attenuation of air temperature cycles below ground surface

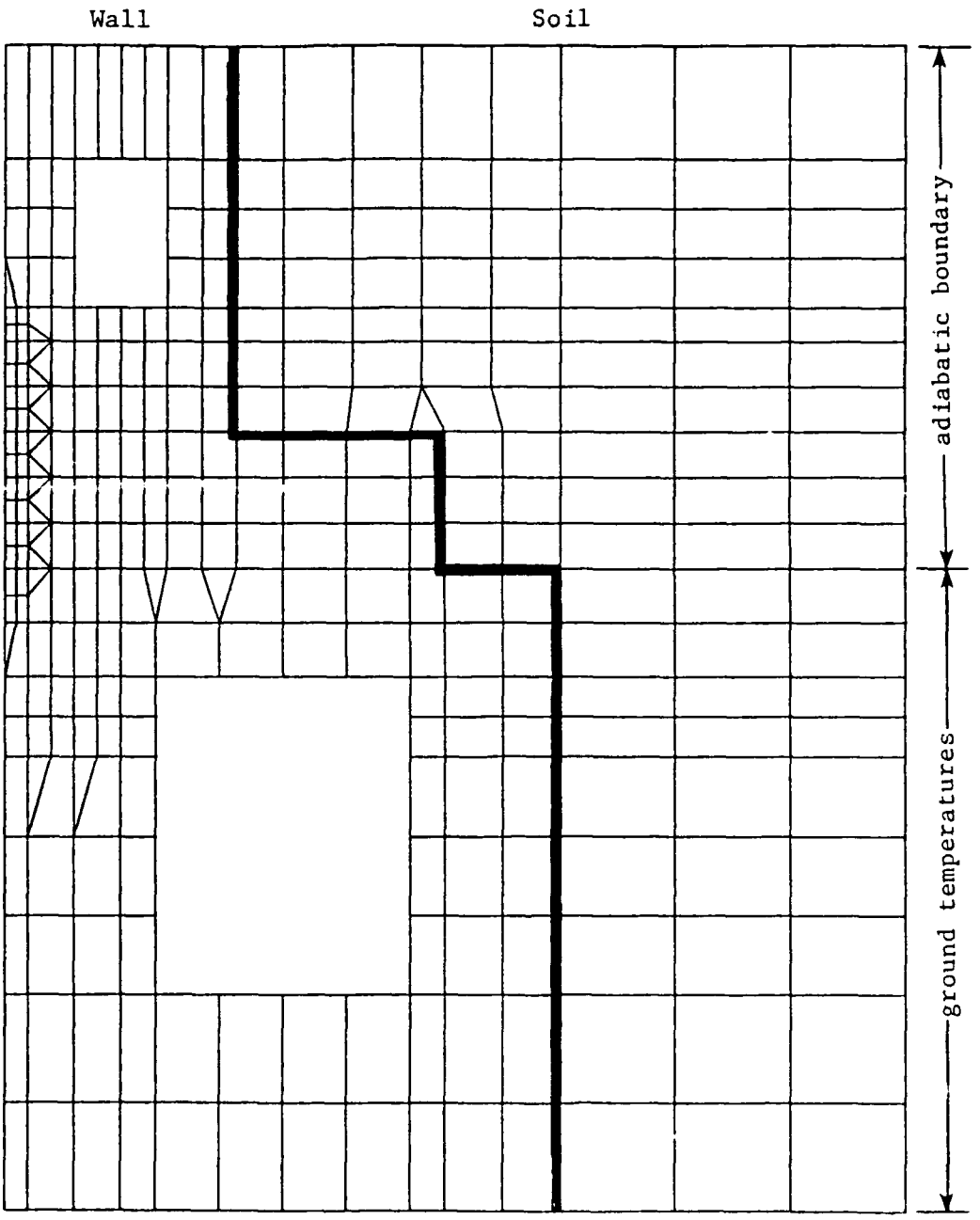

Figure 32. Thermal finite-element model of land wall

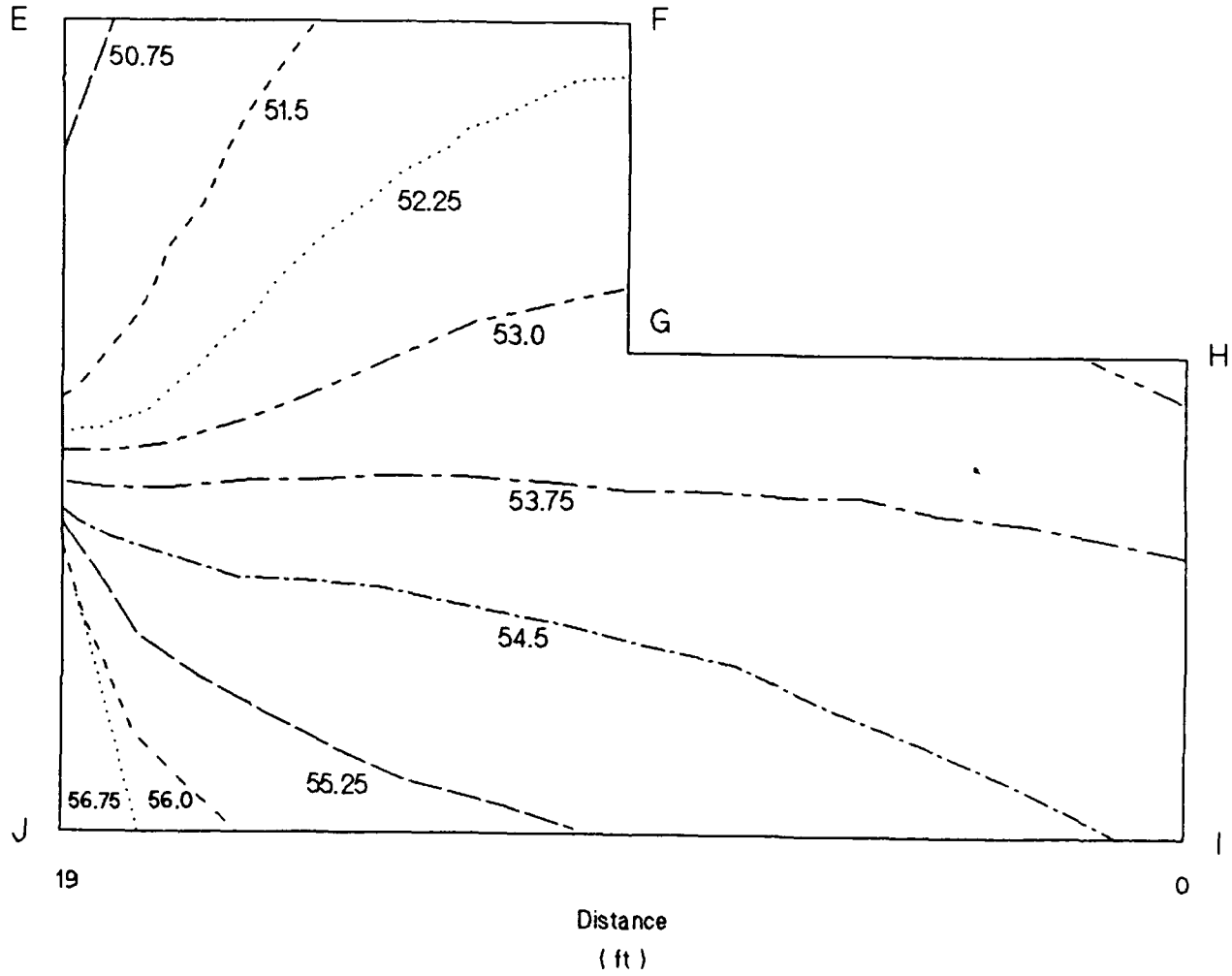

Figure 33. Mean temperatures (°F) in land wall.
See Figure 30 for orientation of this section

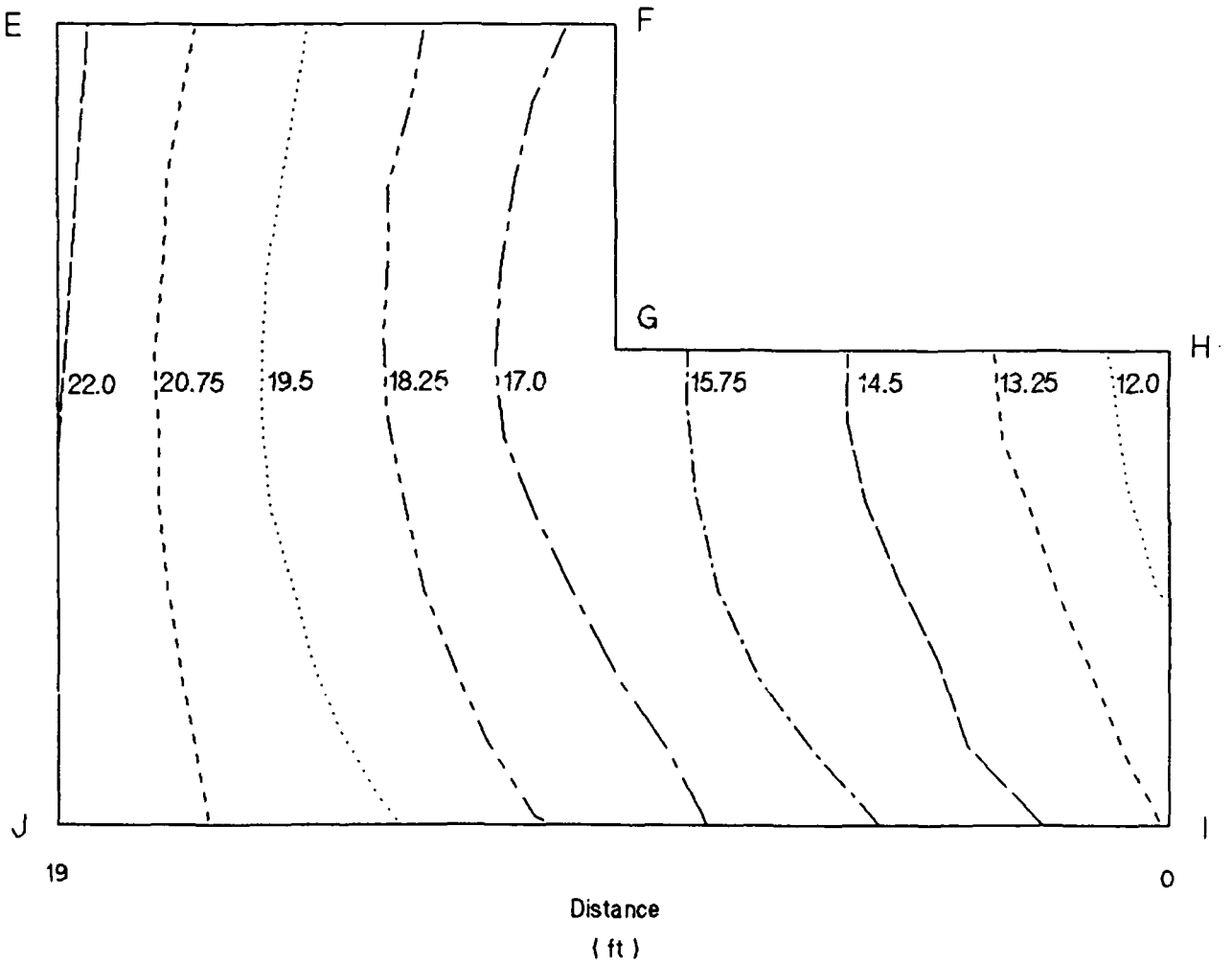

Figure 34. Temperature (°F) amplitudes in land wall.
See Figure 30 for orientation of this section

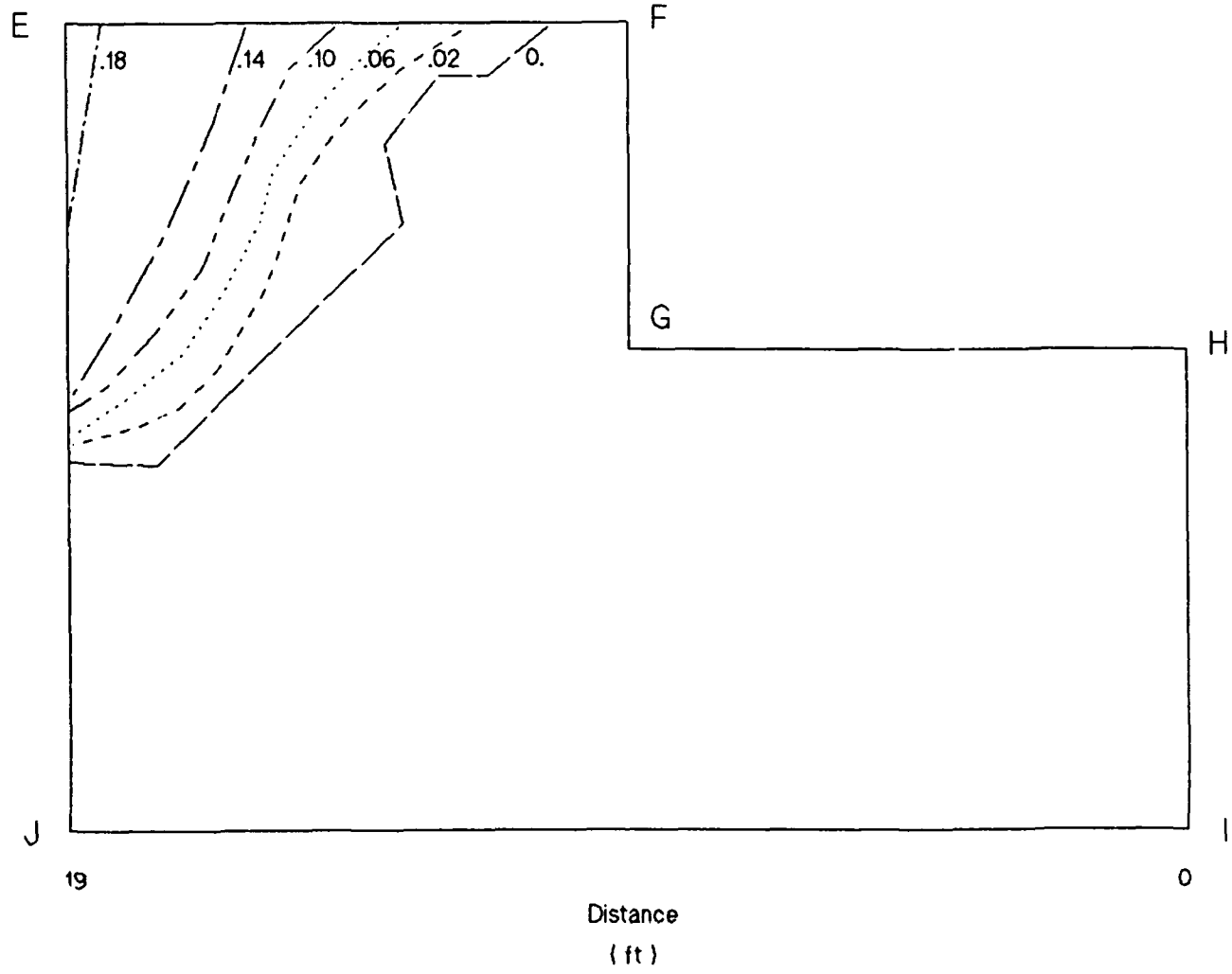

Figure 35. Probability of freezing in land wall.
See Figure 30 for orientation of this section

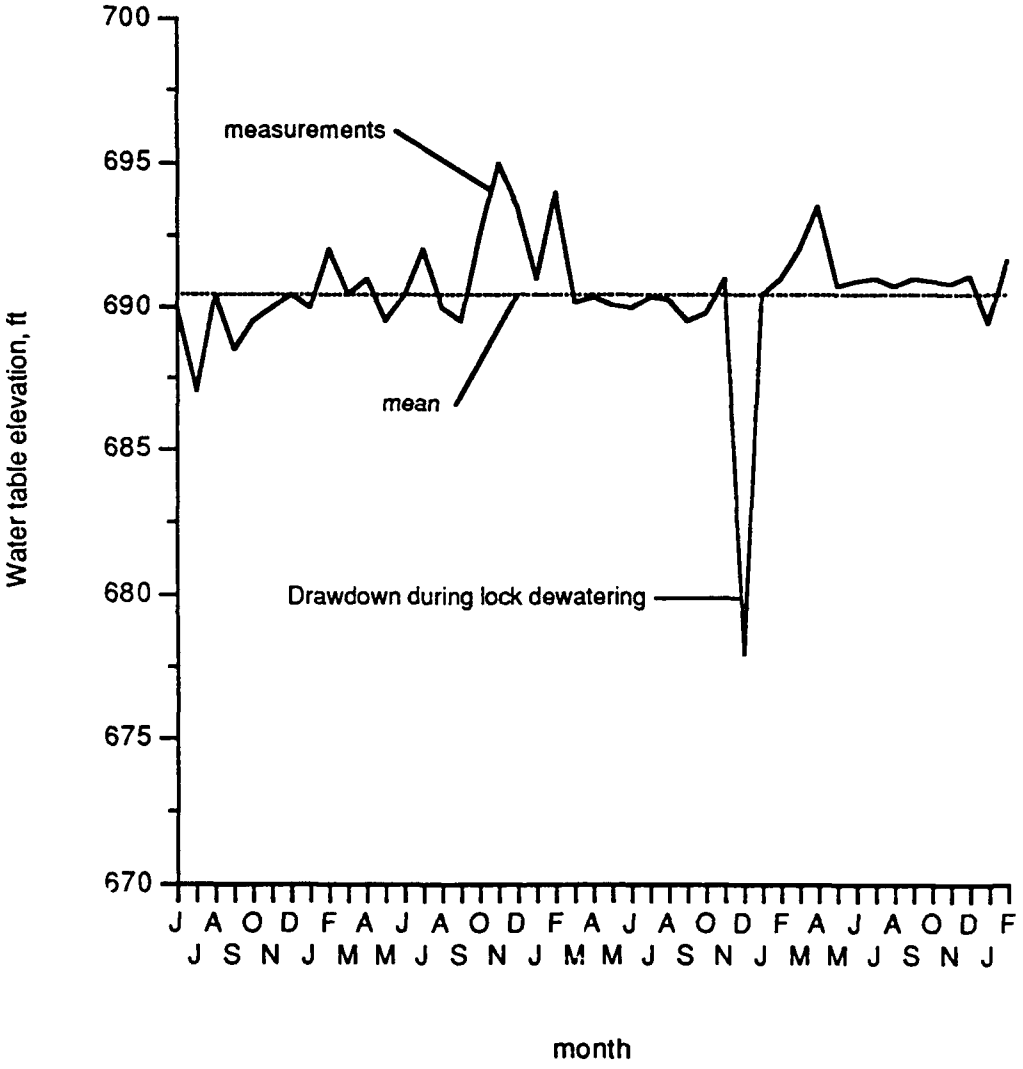

Figure 36. Water table on land side of land wall

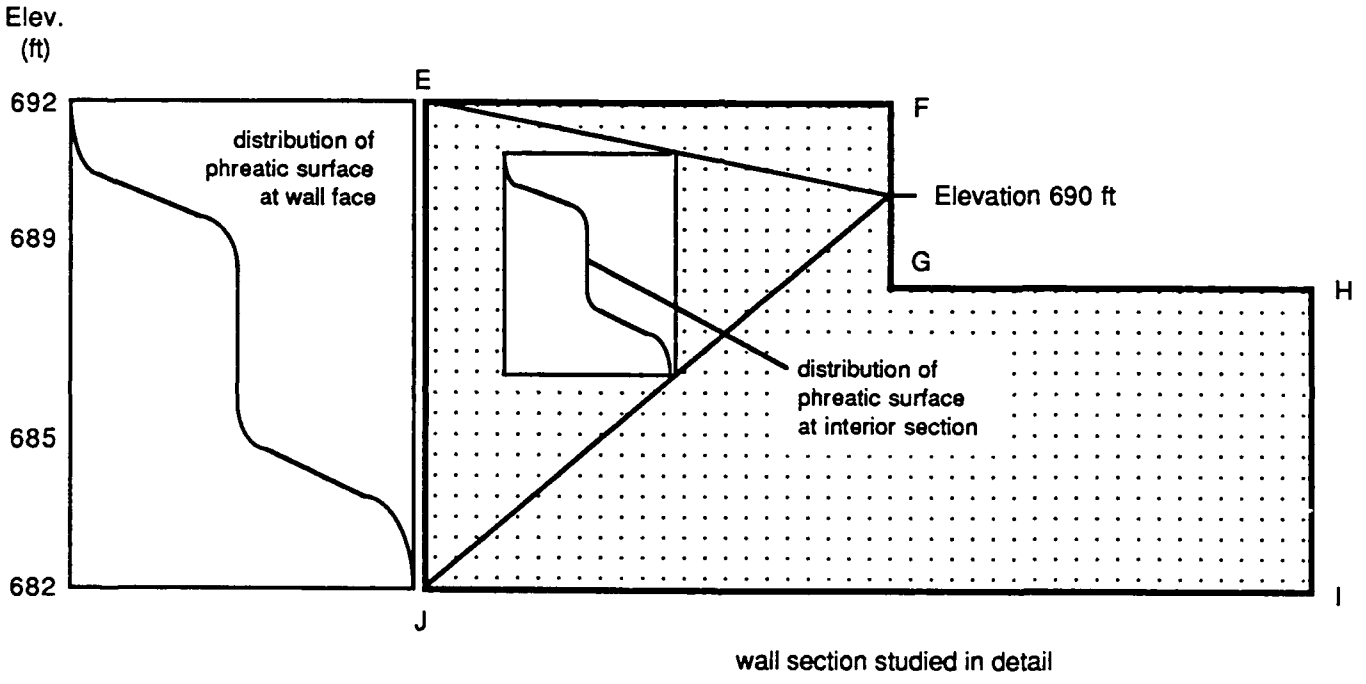

Figure 37. Distribution of phreatic surface in land wall

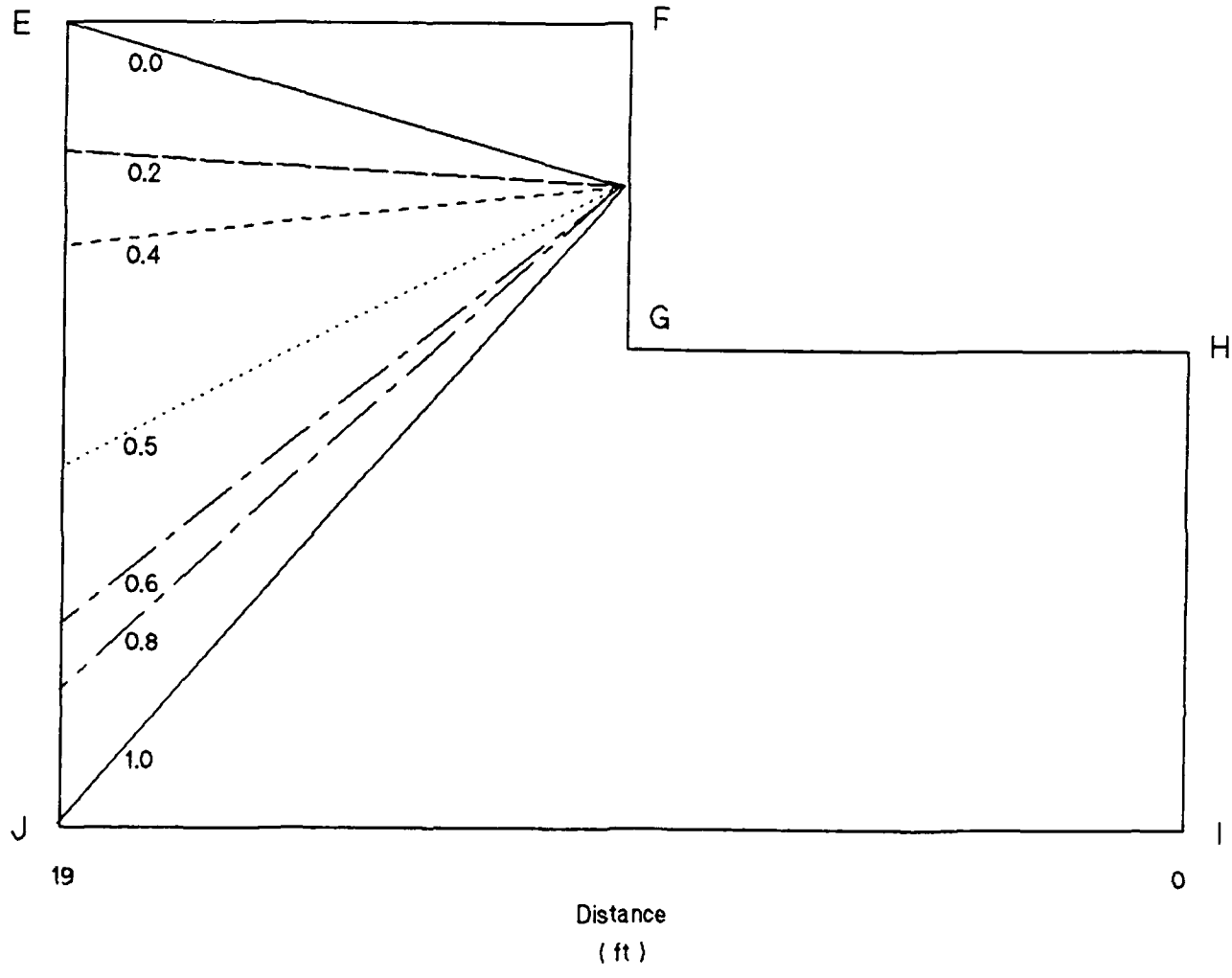

Figure 38. Probability of critical saturation in land wall.
See Figure 30 for orientation of this section

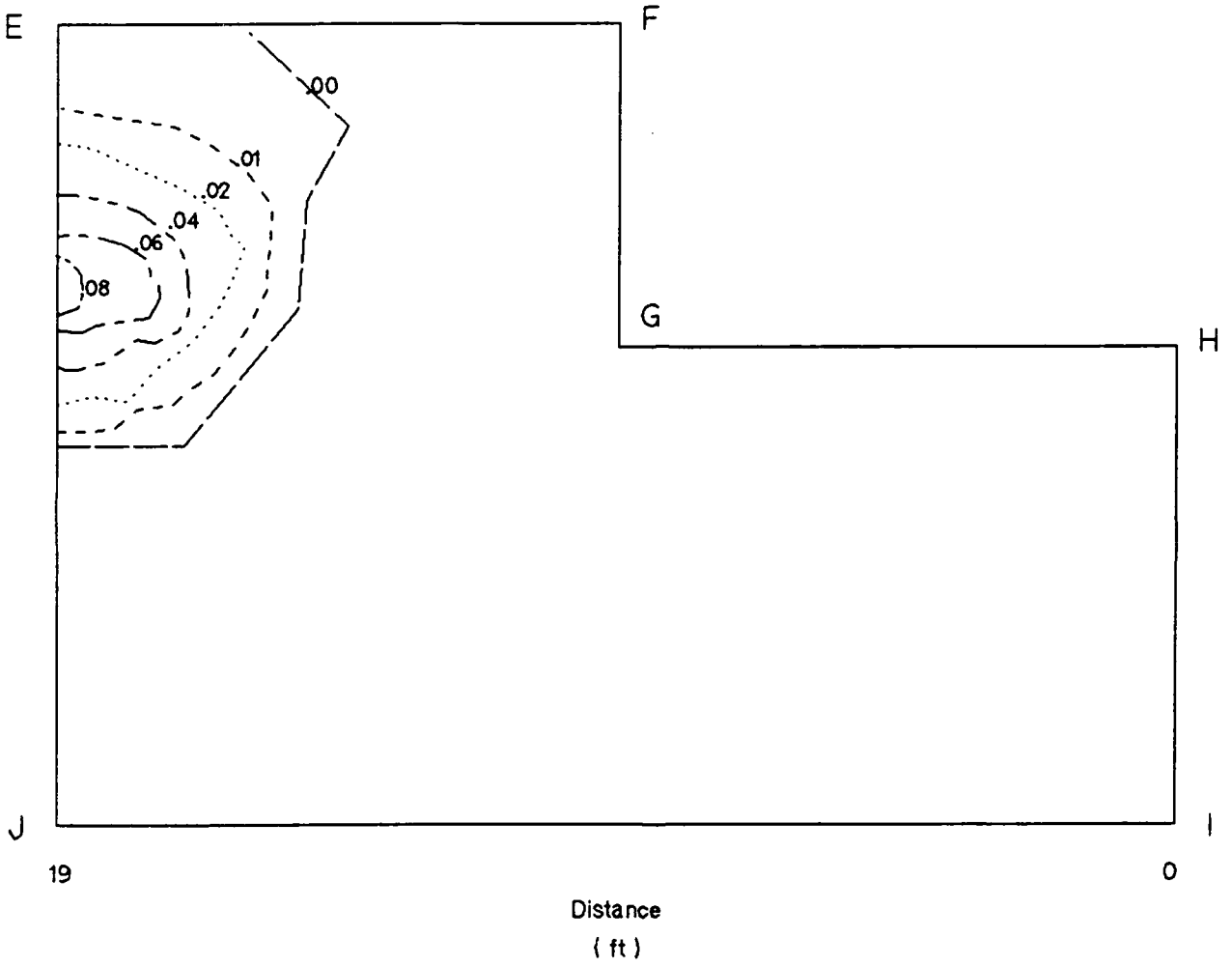

Figure 39. Annual probability of damage for land wall at Dashields Lock. See Figure 30 for orientation of this section

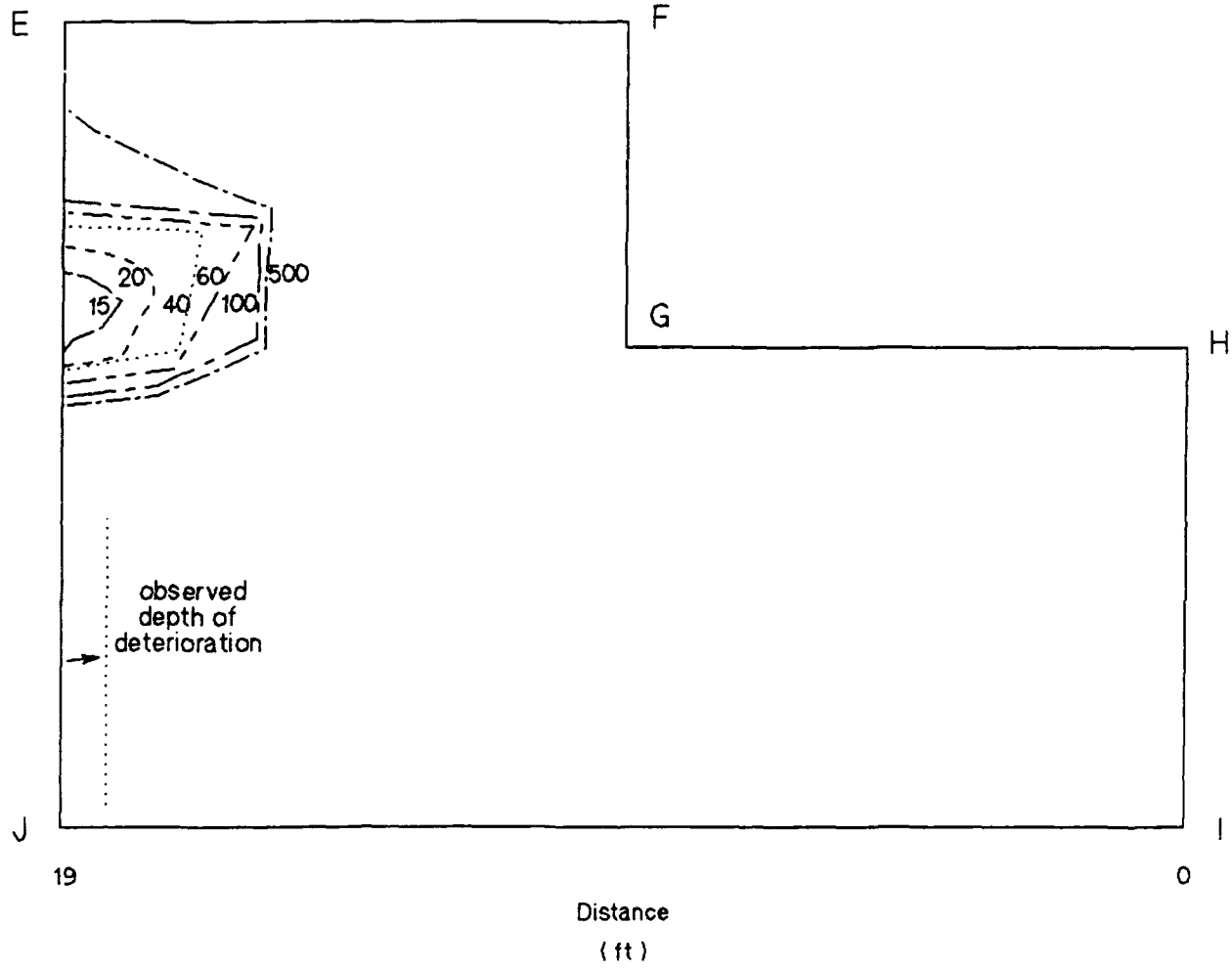

Figure 40. Service life (yrs) prediction for land wall at Dashields Lock. See Figure 30 for orientation of this section

APPENDIX A: SINUSOIDAL CURVE FITTING

For cyclic data with "n" data points evenly spaced over a period "T" and an equation of the form:

$$X(t) = A + B \sin\omega t + C \cos\omega t \ , \ \omega = 2\pi/T$$

the coefficients A, B, and C can be determined by minimizing

$$\Sigma \ [(X_i - (A + B \sin\omega t_i + C \cos\omega t_i)]^2$$

The linear regression equations may be written as

$$\begin{bmatrix} n & \Sigma\sin\omega t_i & \Sigma\cos\omega t_i \\ \Sigma\sin\omega t_i & \Sigma\sin^2\omega t_i & \Sigma\cos\omega t_i \sin\omega t_i \\ \Sigma\cos\omega t_i & \Sigma\cos\omega t_i \sin\omega t_i & \Sigma\cos^2\omega t_i \end{bmatrix} \begin{bmatrix} A \\ B \\ C \end{bmatrix} = \begin{bmatrix} \Sigma X_i \\ \Sigma X_i \sin\omega t_i \\ \Sigma X_i \cos\omega t_i \end{bmatrix}$$

Noting the following simplifications for this case:

$$\Sigma\sin\omega t_i = \Sigma\cos\omega t_i = \Sigma\cos\omega t_i \sin\omega t_i = 0$$
$$\Sigma\sin^2\omega t_i = \int\sin^2\omega t\,dt = T/2$$
$$\Sigma\cos^2\omega t_i = \int\cos^2\omega t\,dt = T/2$$

the coefficients are determined as

$$A = (\Sigma X_i)/n = \text{mean}$$
$$B = (2/T)\Sigma X_i \sin\omega t_i$$
$$C = (2/T)\Sigma X_i \cos\omega t_i$$

For the alternate equation of the form:

$$X(t) = A + D \sin(\omega t + \phi)$$

then

$$D = (B^2 + C^2)^{1/2}$$
$$\phi = \tan^{-1}(B/C)$$

APPENDIX B: SAMPLE CALCULATIONS FOR TEMPERATURE DISTRIBUTION

1-D Temperature Distribution - Sample Calculation

Determine at depth of 6" (0.5 ft) for ambient air temperatures.

Surface temperature $\theta_s = \theta_e e^{i\omega t} = A + D \sin \omega t$

$\bar{A} = 50.275°$ $\quad \sigma_A = 0.768°$ $\quad L = 24$ ft

$\bar{D} = 22.637°$ $\quad \sigma_D = 0.314°$ $\quad \omega = 2\pi/365$

$\bar{h}^2 = 1.20$ ft^2/day $\quad \sigma_{h^2} = 0.20$

Deterministic Temperatures @ $x = 0.5$ ft.

$$\theta(x) = A + X(x)\, D \sin \omega t$$

$$k^2 = \omega/2h^2 = \frac{2\pi}{365(2h^2)} = \frac{1}{116.18\ h^2}$$

$h^2 = 1.2$, $\quad k = 0.08864$ $\quad kL = 2.12737$ $\quad kL' = -2.03874$

$h^2 = 1.0$, $\quad k = 0.09277$ $\quad kL = 2.22659$ $\quad kL' = -2.13381$

$h^2 = 1.4$, $\quad k = 0.07841$ $\quad kL = 1.88181$ $\quad kL' = -1.8034$

$$X(h^2=1.2) = \sqrt{\frac{\cosh(-2.03874) + \cos(-2.03874)}{\cosh(2.12737) + \cos(2.12737)}} = \sqrt{\frac{3.4545}{3.7277}} = 0.96266$$

$$X(h^2=1.0) = \sqrt{\frac{\cosh(-2.13381) + \cos(-2.13381)}{\cosh(2.22659) + \cos(2.22659)}} = 0.95878$$

$$X(h^2=1.4) = \sqrt{\frac{\cosh(-1.8034) + \cos(-1.8034)}{\cosh(1.88181) + \cos(1.88181)}} = 0.96586$$

SAMPLE CALCULATION

Taylor Series Expansion:

$$\theta_o(x) = \theta_o(\bar{h}, \bar{A}, \bar{D}) = 50.275°$$

$$\theta_a(x) = \theta_o(\bar{h}, \bar{A}, \bar{D}) = \bar{X}(x) \cdot \bar{D} = 0.96266(22.637) = 21.79°$$

$$\sigma_o^2(x) = \sigma_A^2 = 0.768^2 = 0.590°$$

$$\theta_a(\bar{D} + \sigma_D) = \bar{X}(x)(D + \sigma_D) = 0.96266(22.95) = 22.093°$$

$$\theta_a(\bar{D} - \sigma_o) = \bar{X}(x)(D - \sigma_D) = 0.96266(22.323) = 21.489°$$

$$\theta_a(\bar{h}^2 + \sigma_{h^2}) = X(h^2 = 1.4)\,\bar{D} = .96586(22.637) = 21.864°$$

$$\theta_a(\bar{h}^2 - \sigma_{h^2}) = X(h^2 = 1.0)\,\bar{D} = .95878(22.637) = 21.704°$$

$$\sigma_a^2 = \left[\left(\frac{\theta_a(D^+) - \theta_a(D^-)}{2} \right)^2 + \left(\frac{\theta_a(h^+) - \theta_a(h^-)}{2} \right)^2 \right] = 0.0976$$

Temperature Distribution:

$$\bar{\theta} = \theta_o(x) = 50.275°$$

$$\sigma_\theta^2 = \sigma_o^2 + \tfrac{1}{2}(\sigma_a^2 + \theta_a^2)$$

$$= .59 + \tfrac{1}{2}(.0976 + 21.79^2) = 238.04°$$

$$\sigma_\theta = 15.43°$$

Table B-1

One dimensional temperature distribution above waterline

dist. X	annual mean So^2	Var(amplitude) .5*Sa^2	mean amplitude .5*Ta^2	Variance total St^2	std. dev. St	St^2 divided by total
0.00	0.59	0.05	256.22	256.86	16.03	0.9975
0.25	0.59	0.05	246.52	247.16	15.72	0.9974
0.50	0.59	0.05	237.44	238.07	15.43	0.9974
0.75	0.59	0.04	228.95	229.58	15.15	0.9973
1.00	0.59	0.04	221.01	221.65	14.89	0.9971
1.50	0.59	0.04	206.73	207.36	14.40	0.9970
2.00	0.59	0.04	194.38	195.01	13.96	0.9968
2.50	0.59	0.04	183.77	184.40	13.58	0.9966
3.00	0.59	0.04	174.73	175.36	13.24	0.9964
4.00	0.59	0.04	160.70	161.32	12.70	0.9962
5.00	0.59	0.04	151.07	151.70	12.32	0.9958
6.00	0.59	0.04	144.80	145.43	12.06	0.9957
7.00	0.59	0.04	141.00	141.63	11.90	0.9956
8.00	0.59	0.04	138.92	139.54	11.81	0.9956
9.00	0.59	0.04	137.93	138.55	11.77	0.9955
10.00	0.59	0.04	137.56	138.18	11.76	0.9955
11.00	0.59	0.04	137.47	138.10	11.75	0.9954
12.00	0.59	0.04	137.47	138.09	11.75	0.9955

Table B-2

One dimensional temperature distribution below waterline

dist. X	annual mean So^2	Var(amplitude) .5*Sa^2	mean amplitude .5*Ta^2	Variance total St^2	std. dev. St	St^2 divided by total
0.00	3.87	0.01	244.42	248.30	15.76	0.9844
0.25	3.87	0.01	235.17	239.05	15.46	0.9838
0.50	3.87	0.01	226.51	230.38	15.18	0.9832
0.75	3.87	0.01	218.40	222.28	14.91	0.9825
1.00	3.87	0.01	210.84	214.72	14.65	0.9819
1.50	3.87	0.01	197.21	201.09	14.18	0.9807
2.00	3.87	0.01	185.43	189.31	13.76	0.9795
2.50	3.87	0.01	175.31	179.19	13.39	0.9783
3.00	3.87	0.01	166.68	170.56	13.06	0.9773
4.00	3.87	0.01	153.30	157.18	12.54	0.9753
5.00	3.87	0.01	144.11	148.00	12.17	0.9737
6.00	3.87	0.01	138.14	142.02	11.92	0.9727
7.00	3.87	0.01	134.51	138.39	11.76	0.9720
8.00	3.87	0.01	132.52	136.40	11.68	0.9716
9.00	3.87	0.01	131.57	135.46	11.64	0.9713
10.00	3.87	0.01	131.22	135.11	11.62	0.9712
11.00	3.87	0.01	131.14	135.03	11.62	0.9712
12.00	3.87	0.01	131.14	135.02	11.62	0.9713